

Dinuclear Dicyclopentadienyl Titanium Complexes with Bridging Cyclopentadienylsiloxo Ligands

Lorena Postigo,[†] Luca Bellarosa,[‡] Javier Sánchez-Nieves,[†] Pascual Royo,^{*,†}
Agustí Lledós,^{*,‡,§} and Marta E. G. Mosquera^{†,§}

[†]Departamento de Química Inorgánica, Universidad de Alcalá, Campus Universitario, E-28871 Alcalá de Henares (Madrid), Spain and [‡]Departament de Química, Universitat Autònoma de Barcelona, E-08193 Bellaterra (Barcelona), Spain. [§]X-ray diffraction studies.

Received October 26, 2009

Addition of 1 equiv of TiCp to compound [(TiCl₂)₂(μ-(η⁵-C₅Me₄SiMeO)₂(μ-O))] (**A**) at 80 °C gave a mixture with different molar ratios of the two possible isomers of [(TiClCp)(TiCl₂)(μ-(η⁵-C₅Me₄SiMeO)₂(μ-O))] (**1**). Reaction of compound **A** with 2 equiv of TiCp at 80 °C afforded [(TiClCp)₂(μ-(η⁵-C₅Me₄SiMeO)₂(μ-O))] (**2as**) as the unique reaction product. Each Cp ligand of **2as** is located in different positions *anti* and *syn* with respect to the Si–O–Si bridge. However, a mixture of two isomers of [(TiClCp)₂(μ-(η⁵-C₅Me₄SiMeO)₂(μ-O))] (**2as** (> 95% by NMR) and **2aa** (< 5% by NMR), was obtained when the reaction was carried out at 60 °C; the two Cp ligands of **2aa** were located at *anti* positions. Alkylation of isomer **2as** with LiMe gave a mixture of the three possible isomers [(TiMeCp)₂(μ-(η⁵-C₅Me₄SiMeO)₂(μ-O))] (**3as**, **3aa**, **3ss**). The proportion of each was dependent on the reaction temperature. Isomer **2as** reacted with Lewis acids E(C₆F₅)₃ (E = B, Al) and with Li[B(C₆F₅)₄] to give the chloro-bridged dititanium compounds [(TiCp)₂(μ-(η⁵-C₅Me₄SiMeO)₂(μ-O))(μ-Cl)][Q] (Q = ClB(C₆F₅)₃, **4B**; ClAl(C₆F₅)₃, **4A**; Q = B(C₆F₅)₄, **4C**) as the unique reaction products. Addition of [Ph₃C][B(C₆F₅)₄] to the mixture of isomers in **3** gave a mixture of complexes [(TiCpMe)(TiCp)(μ-(η⁵-C₅Me₄SiMeO)₂(μ-O))][Q] (**5aC** and **5sC**; Q = B(C₆F₅)₄), with the remaining methyl ligand located at *anti* or *syn* positions depending on the methyl group being abstracted. DFT studies were carried out to determine the stability of the isomers of **2** and **3**, to determine which chlorine atom in compound **2as** was more easily eliminated, and also to clarify the transformation of isomer **2as** into the mixture of isomers **3as**, **3aa**, and **3ss** during the alkylation reaction.

Introduction

The design of ligands to generate bimetallic systems has been developed with the aim of finding reactivity patterns different from those observed for similar monometallic complexes.¹ In this regard, the cooperative effect between the metal atoms in group 4 dinuclear complexes has been shown to induce important modifications in polymerization

behavior with respect to related mononuclear systems.^{2–18} Although this cooperative effect is well documented, dicationic dinuclear group 4 complexes are mainly obtained from cationic mononuclear derivatives.^{19–22}

Functionalization of cyclopentadienyl rings with chlorosilyl groups^{23–30} has provided a particularly useful procedure to

*Corresponding authors. Fax: 00 34 93 581 2920. E-mail: pascual.royo@uah.es; agusti@klingon.uab.es.

- (1) Gavrilova, A. L.; Bosnich, B. *Chem. Rev.* **2004**, *104*, 349.
- (2) Salata, M. R.; Marks, T. J. *Macromolecules* **2009**, *42*, 1920.
- (3) Motta, A.; Fragala, I. L.; Marks, T. J. *J. Am. Chem. Soc.* **2009**, *131*, 3974.
- (4) Salata, M. R.; Marks, T. J. *J. Am. Chem. Soc.* **2008**, *130*, 12.
- (5) Guo, N.; Stern, C. L.; Marks, T. J. *J. Am. Chem. Soc.* **2008**, *130*, 2246.
- (6) Lee, S. H.; Wu, C. J.; Joung, U. G.; Lee, B. Y.; Park, J. *Dalton Trans.* **2007**, 4608.
- (7) Lee, M. H.; Kim, S. K.; Do, Y. *Organometallics* **2005**, *24*, 3618.
- (8) Stojcevic, G.; Kim, H.; Taylor, N. J.; Marder, T. B.; Collins, S. *Angew. Chem., Int. Ed.* **2004**, *43*, 5523.
- (9) Guo, N.; Li, L. T.; Marks, T. J. *J. Am. Chem. Soc.* **2004**, *126*, 6542.
- (10) Sierra, J. C.; Huerlander, D.; Hill, M.; Kehr, G.; Erker, G.; Fröhlich, R. *Chem.—Eur. J.* **2003**, *9*, 3618.
- (11) Noh, S. K.; Lee, J.; Lee, D. H. *J. Organomet. Chem.* **2003**, *667*, 53.
- (12) Alt, H. G.; Ernst, R. *J. Mol. Catal. A: Chem.* **2003**, *195*, 11.

- (13) Alt, H. G.; Ernst, R. *Inorg. Chim. Acta* **2003**, *350*, 1.
- (14) Li, L. T.; Metz, M. V.; Li, H. B.; Chen, M. C.; Marks, T. J.; Liable-Sands, L.; Rheingold, A. L. *J. Am. Chem. Soc.* **2002**, *124*, 12725.
- (15) Alt, H. G.; Ernst, R.; Bohmer, I. K. *J. Organomet. Chem.* **2002**, *658*, 259.
- (16) Noh, S. K.; Kim, J.; Jung, J.; Ra, C. S.; Lee, D.-h.; Lee, H. B.; Lee, S. W.; Huh, W. S. *J. Organomet. Chem.* **1999**, *580*, 90.
- (17) Chen, Y. X.; Metz, M. V.; Li, L. T.; Stern, C. L.; Marks, T. J. *J. Am. Chem. Soc.* **1998**, *120*, 6287.
- (18) Li, Y. F.; Ward, D. G.; Reddy, S. S.; Collins, S. *Macromolecules* **1997**, *30*, 1875.
- (19) Chen, M. C.; Roberts, J. A. S.; Seyam, A. M.; Li, L.; Zuccaccia, C.; Stahl, N. G.; Marks, T. J. *Organometallics* **2006**, *25*, 2833.
- (20) Lian, B.; Toupet, L.; Carpentier, J.-F. *Chem.—Eur. J.* **2004**, *10*, 4301.
- (21) Sadow, A. D.; Tilley, T. D. *J. Am. Chem. Soc.* **2003**, *125*, 9462.
- (22) Yang, X.; Stern, C. L.; Marks, T. J. *J. Am. Chem. Soc.* **1994**, *116*, 10015.
- (23) Postigo, L.; Sánchez-Nieves, J.; Royo, P. *Inorg. Chim. Acta* **2007**, *360*, 1305.
- (24) Santamaría, D.; Cano, J.; Royo, P.; Mosquera, M. E. G.; Cuenca, T.; Frutos, L. M.; Castaño, O. *Angew. Chem., Int. Ed.* **2005**, *44*, 5828.

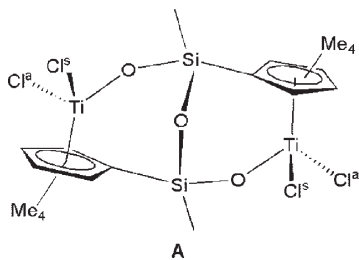


Figure 1. Diagram of complex **A** labeling the two different *anti* (Cl^a) and *syn* (Cl^s) positions at the Ti atom with respect to the orientation of the Si–O–Si bridge.

synthesize dinuclear compounds through hydrolysis of the Si–Cl bonds.^{25,30–36} Following this procedure, the hydrolysis of the dichlorosilyl-cyclopentadienyl titanium compound $[\text{Ti}\{\eta^5\text{-C}_5\text{Me}_4(\text{SiMeCl}_2)\}\text{Cl}_2]^{26}$ allowed us to obtain the dititanium derivative $[(\text{TiCl}_2)_2(\mu\text{-}\{\eta^5\text{-C}_5\text{Me}_4\text{SiMeO}\}_2(\mu\text{-O}))]$ (**A**) with both Si–O–Si and Si–O–Ti bridges (Figure 1).³⁷

The intrinsically diastereoselective formation of the Si–O–Si bridge is responsible for the generation of only one C_2 symmetry diastereoisomer of **A** despite the presence of two diastereogenic Si atoms. Furthermore, the Si–O–Si bridge causes the two chlorine atoms to occupy different positions, one toward the bridge (*syn* position) and the other away from it (*anti* position).

Complex **A** has two potentially active metal centers for olefin polymerization. However, we observed in previous works that the ease of formation of bridges caused complex **A** to be inactive for ethylene polymerization, although the methyl derivative $[(\text{TiMe}_2)_2(\mu\text{-}\{\eta^5\text{-C}_5\text{Me}_4\text{SiMeO}\}_2(\mu\text{-O}))]$ was active for MMA polymerization.³⁷ Incomplete abstraction of two alkyl groups was possible only in the reaction of the benzyl derivative $[(\text{TiBz}_2)_2(\mu\text{-}\{\eta^5\text{-C}_5\text{Me}_4\text{SiMeO}\}_2(\mu\text{-O}))]$ with excess $\text{B}(\text{C}_6\text{F}_5)_3$ for several days.³⁷ We synthesized dialkoxo-bridged complexes $[(\text{TiX})_2(\mu\text{-O}_2\text{L})(\mu\text{-}\{\eta^5\text{-C}_5\text{Me}_4\text{SiMeO}\}_2(\mu\text{-O}))]$ ($\text{X} = \text{Cl, Me, Bz}$) to avoid the formation of halide or alkyl bridges between the metal centers, thus favoring the generation of dicationic dinuclear compounds.³⁸ Once again, we were unable to characterize any dicationic compounds, and only monocationic dinuclear

derivatives were isolated. However, polymerization of ϵ -caprolactone with $[\{\text{Ti}(\text{O}i\text{Pr})_2\}_2(\mu\text{-}\{\eta^5\text{-C}_5\text{Me}_4\text{SiMeO}\}_2(\mu\text{-O}))]$ was influenced by the cooperative effect of both metal atoms, obtaining PCL with double the M_w of that obtained with a related mononuclear compound.³⁸

In this paper we report our ongoing research on dinuclear compounds with bridging cyclopentadienylsiloxo ligands derived from compound **A** (Figure 1). New dinuclear dicyclopentadienyl complexes have been synthesized, and their reactivity with different molar ratios of Lewis acids has been explored, as the dinuclear nature of these new compounds could aid the synthesis of dinuclear dicationic derivatives.

Results and Discussion

Reactions of A with TICp. Reaction of compound **A** with 1 equiv of TICp in toluene at 80 °C for 48 h afforded a mixture containing unreacted complex **A** (25% by ^1H NMR) together with a very small amount of the dicyclopentadienyl derivative **2as** (8% by ^1H NMR) and a mixture of two components corresponding to the two possible isomers of the monosubstituted dinuclear compound $[(\text{TiClCp})(\text{TiCl}_2)(\mu\text{-}\{\eta^5\text{-C}_5\text{Me}_4\text{SiMeO}\}_2(\mu\text{-O}))]$ (**1 anti** and *syn*) (Scheme 1). These two components containing the Cp ring located at the *syn* or *anti* positions with respect to the orientation of the Si–O–Si bridge are present in significantly different molar ratios (major isomer 50% by ^1H NMR; minor isomer 17% by ^1H NMR). Although unfortunately we could not assign the *syn* and *anti* isomers to the major and minor isomer components of this mixture, it is clear that the introduction of the first cyclopentadienyl ligand in compound **A** is a ca. 75% regioselective reaction for one preferred position. The ^1H and ^{13}C NMR spectra of this mixture are consistent with the presence of two compounds that are asymmetric molecules, and each shows eight resonances for two $\text{C}_5\text{Me}_4\text{Si}$ rings, two resonances for both SiMe groups, and one for the Cp ligand.

Reaction of $[(\text{TiCl}_2)_2(\mu\text{-}\{\eta^5\text{-C}_5\text{Me}_4\text{SiMeO}\}_2(\mu\text{-O}))]$ (**A**) with 2 equiv of TICp in toluene at 80 °C gave $[(\text{TiClCp})_2(\mu\text{-}\{\eta^5\text{-C}_5\text{Me}_4\text{SiMeO}\}_2(\mu\text{-O}))]$ (**2as**) as the only titanium product in high yield (Scheme 1). The Cp ligands of **2as** are located at opposite *anti*–*syn* positions with respect to the Si–O–Si bridge, corresponding to the more stable isomer, as this orientation probably minimizes steric repulsions (*vide infra*). Compound **2as** is an asymmetric molecule, and thus, its ^1H and ^{13}C NMR spectra showed eight resonances for two $\text{C}_5\text{Me}_4\text{Si}$ rings and two resonances for both SiMe groups and also for both Cp ligands. The relative position *anti*–*syn* for each Cp ligand was determined by NOE NMR experiments (Figure 2), taking into account that the structures of complexes **A** and **2aa** show that the ligand at the *syn* position is closer to the SiMe group of the Ti–O–Si moiety to which this Cp ligand is bound.

Therefore, introduction of the second cyclopentadienyl ligand at 80 °C is regiospecific, as this second ligand is always located opposite the first Cp ligand, regardless of its previous position with respect to the Si–O–Si bridge.

However, a mixture of two isomers of $[(\text{TiClCp})_2(\mu\text{-}\{\eta^5\text{-C}_5\text{Me}_4\text{SiMeO}\}_2(\mu\text{-O}))]$ was obtained when the reaction of **A** with 2 equiv of TICp was carried out at 60 °C. This mixture contains the isomer **2as** as the major component (> 95% by NMR) along with a very small amount (< 5% by NMR) of a second component identified as the **2aa** isomer. Compound **2aa** showed both Cp ligands located at the *anti* positions. The ^1H NMR spectrum of this mixture showed, apart from

(25) Arteaga-Müller, R.; Sánchez-Nieves, J.; Royo, P.; Mosquera, M. E. G. *Polyhedron* **2005**, *24*, 1274.

(26) Vázquez, A. B.; Royo, P.; Herdtweck, E. *J. Organomet. Chem.* **2003**, *683*, 155.

(27) Vázquez, A. B.; Royo, P. *J. Organomet. Chem.* **2003**, *671*, 172.

(28) Cano, J.; Royo, P.; Lanfranchi, M.; Pellinghelli, M. A.; Tiripicchio, A. *Angew. Chem., Int. Ed.* **2001**, *40*, 2495.

(29) Alcalde, M. I.; Gómez-Sal, M. P.; Royo, P. *Organometallics* **1999**, *18*, 546.

(30) Alcalde, M. I.; Gómez-Sal, P.; Martín, A.; Royo, P. *Organometallics* **1998**, *17*, 1144.

(31) Buitrago, O.; Jiménez, G.; Cuenca, T. *J. Organomet. Chem.* **2003**, *683*, 70.

(32) Alcalde, M. I.; Gómez-Sal, M. P.; Royo, P. *Organometallics* **2001**, *20*, 4623.

(33) Park, J. T.; Yoon, S. C.; Bae, B. J.; Seo, W. S.; Suh, I. H.; Han, T. K.; Park, J. R. *Organometallics* **2000**, *19*, 1269.

(34) de la Mata, F. J.; Giner, P.; Royo, P. *J. Organomet. Chem.* **1999**, *572*, 155.

(35) Ciruelos, S.; Cuenca, T.; Gómez, R.; Gómez-Sal, P.; Manzanero, A.; Royo, P. *Organometallics* **1996**, *15*, 5577.

(36) Ciruelos, S.; Cuenca, T.; Gómez-Sal, P.; Manzanero, A.; Royo, P. *Organometallics* **1995**, *14*, 177.

(37) Postigo, L.; Vázquez, A. B.; Sánchez-Nieves, J.; Royo, P.; Herdtweck, E. *Organometallics* **2008**, *27*, 5588.

(38) Postigo, L.; Sánchez-Nieves, J.; Royo, P.; Mosquera, M. E. G. *Dalton Trans.* **2009**, 3756.

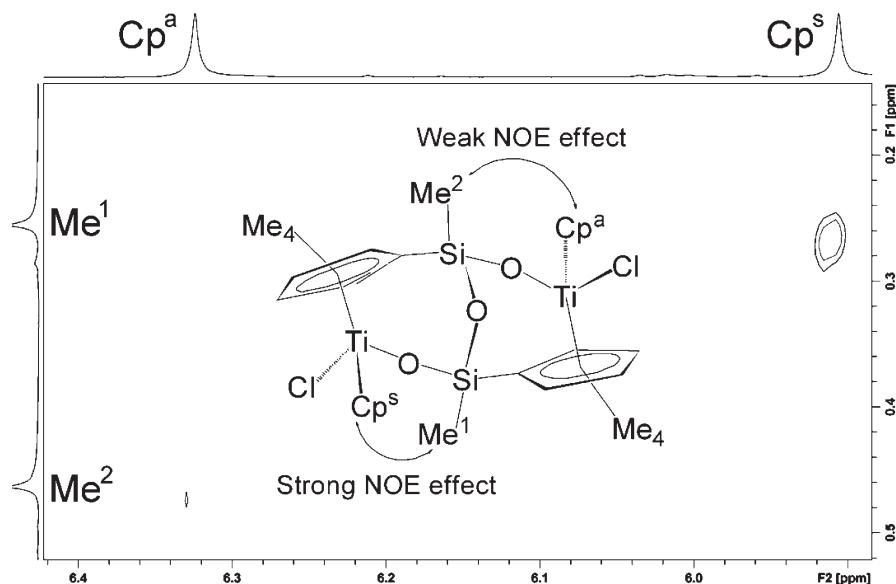
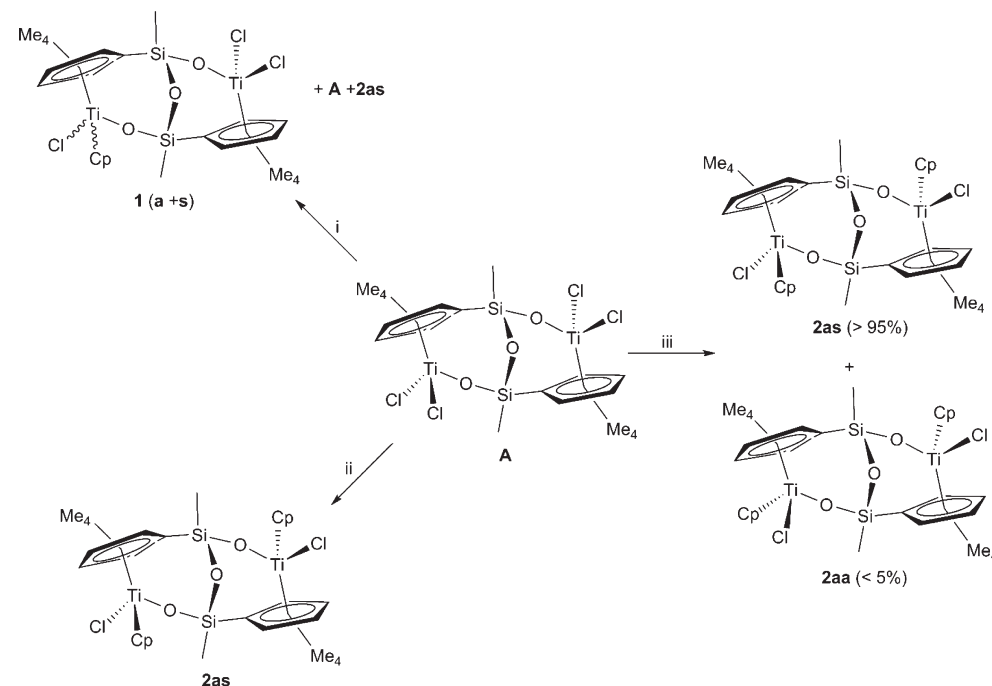


Figure 2. 2D NOE NMR spectrum of compound **2as** showing the interactions between Cp ligands and SiMe groups.

Scheme 1^a



^a (i) TICp, 80 °C; (ii) 2 TICp, 80 °C; (iii) 2 TICp, 60 °C.

the resonances belonging to **2as**, new resonances corresponding to the new C_2 symmetry isomer **2aa**, which contains two equivalent asymmetric titanium units. Thus, four resonances for two equivalent C_5Me_4Si rings, one for both SiMe groups, and one for both equivalent Cp ligands were observed. Fortunately, single crystals of **2aa** suitable for X-ray diffraction studies were obtained from a toluene solution of the mixture cooled at -40 °C, whereas appropriate crystals of **2as** could not be isolated and formation of the remaining possible isomer **2ss** was not detected.

The molecular structure of **2aa** is illustrated in Figure 3, and selected bond lengths and angles are listed in Table 1, as well as those obtained by theoretical calculations (see below). The molecular structure of **2aa** consists of a dinuclear

molecule formed by two Ti atoms connected by two bridging $[\mu-(\eta^5-C_5R_4SiMeO)]$ fragments, with each of Ti atoms bound to one bridging $\eta^5-C_5Me_4Si$ ring and to the oxygen atom of a similar second bridging fragment. One additional oxygen atom also links both bridges through the Si atoms, retaining the initial geometry of compound **A**.³⁷ Furthermore, both Ti atoms are also bound to one Cp and one Cl ligand. Both Cp and Cl ligands occupy equivalent positions in the molecule. The environment about each Ti atom corresponds to the typical pseudotetrahedral dicyclopentadienyl geometry.^{39,40}

(39) Thiele, K.-H.; Gerstner, P.; Somoza, F. *Z. Anorg. Allg. Chem.* **2001**, *627*, 28.

(40) Grimmond, B. J.; Corey, J. Y.; Rath, N. P. *Acta Crystallogr., Sect. C: Cryst. Struct. Commun.* **2000**, *56*, 53.

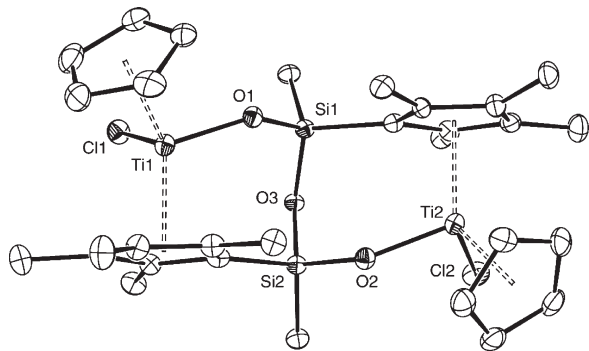


Figure 3. ORTEP plot of the molecular structure of $[(\text{TiCpCl})_2(\mu\text{-}\{\eta^5\text{-C}_5\text{Me}_4\text{SiMeO}\}_2(\mu\text{-O}))]$ (**2aa**) in the solid state. Thermal ellipsoids are drawn at the 30% probability level. Hydrogen atoms are omitted for clarity.

Table 1. Selected Bond Distances (Å) and Angles (deg) for Compound **2aa**^a

bond/angle	experimental		calculated	
	Ti 1	Ti 2	Ti 1	Ti 2
Ti–O	1.903(3)	1.898(4)	1.870	1.864
Ti–Cl	2.397(2)	2.420(2)	2.392	2.391
Ti–Cp'	2.257	2.247	2.291	2.295
Ti–Cp	2.109	2.114	2.126	2.132
Si–O(3)	1.653(4)	1.661(4)	1.674	1.674
Ti···Ti	5.914		5.626	
Si···Si	2.809		2.814	
O–Ti–Cl	93.84(13)	94.77(13)	94.0	94.4
O–Ti–Cp'	119.65	120.09	121.6	121.6
O–Ti–Cp	104.93	104.67	104.7	104.4
Cl–Ti–Cp'	107.83	106.84	102.7	101.7
Cl–Ti–Cp	103.97	103.19	104.0	104.3
Cp'–Ti–Cp	121.92	122.44	123.9	124.4
Ti–O–Si	142.4(2)	144.0(2)	141.6	143.8
Si–O(3)–Si	115.9(2)		114.4	

^a“Experimental” stands for X-ray-determined parameters, whereas “calculated” stands for the DFT-optimized structure. Cp' stands for C₅Me₄Si.

The bond distances and angles within the $[\text{Ti}_2(\mu\text{-}\{\eta^5\text{-C}_5\text{Me}_4\text{SiMeO}\}_2)]$ moiety are very similar to those found for related Si–O–Ti bridged binuclear compounds,^{33,36,41} with or without an additional Si–O–Si bridge, with the exception of the Ti(1)–O–Si(1) angle, which is smaller, and the Ti–OSi bond distance, which is ca. 0.1 Å longer for compounds with this type of Si–O–Si bridging system or with an additional single atom bridging both Ti atoms. The presence of the cyclopentadienyl Cp ligands causes the coplanarity of the $\eta^5\text{-C}_5\text{Me}_4$ rings, as in $[(\text{TiCl}_2)_2(\mu\text{-}\{\eta^5\text{-C}_5\text{R}_4\text{SiMe}_2\text{O}\}_2)]$ (R = H,³⁶ Me³³), and also the elongation of the Ti–Ti distance, which is the longest found in complexes with a $[\text{Ti}_2(\mu\text{-}\{\eta^5\text{-C}_5\text{Me}_4\text{SiMeO}\}_2)]$ moiety and also longer than in the analogous compound $[(\text{TiCl}_2)_2(\mu\text{-}\{\eta^5\text{-C}_5\text{H}_4\text{B}\{\text{NHMe}_2\}\text{O}\}_2(\mu\text{-O}))]$.⁴²

Reaction of 2as with LiMe. Alkylation of the isolated pure isomer **2as** with LiMe in toluene did not give a unique compound but instead gave a mixture containing variable amounts of the three possible isomers of the dimethyl complexes $[(\text{TiMeCp})_2(\mu\text{-}\{\eta^5\text{-C}_5\text{Me}_4\text{SiMeO}\}_2(\mu\text{-O}))]$ (**3**) (Scheme 2;

Scheme 2. Reaction of **2as** with LiMe

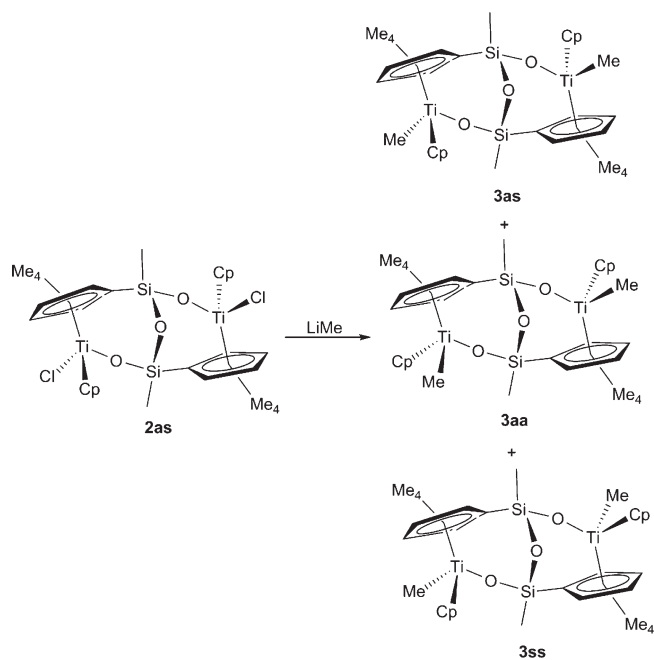


Table 2. Total Yield and Relative Proportion^a of Resulting Isomers from Methylation of **2as** at Variable Temperature

T (°C)	t (h)	3as	3aa	3ss	yield (%)
–78	5	50	50	0	70
0	5	45	45	10	70
25	5	75	15	10	50
50	2	66	0	34	30

^aDetermined by ¹H NMR spectroscopy.

Table 2), depending on the temperature conditions. The yield was also dependent on the temperature (Table 2). Higher total yields were obtained at lower temperatures, indicating that thermal decomposition of any reaction intermediates probably takes place at higher temperatures; the starting complex **2as** and the mixture of isomers of **3** were stable when heated for several hours in toluene. The isomer **3as** with both Cp groups located at opposite *anti-syn* positions with respect to the Si–O–Si bridge is always the major component of the mixture, regardless of the reaction temperature, although at –78 °C it is formed in the same proportion as isomer **3aa** with both Cp substituents located at *anti* positions. The proportion of isomer **3aa** decreases at increasing temperatures and is absent at 50 °C, whereas simultaneously the proportion of isomer **3ss**, with both methyl groups located at *anti* positions, increases and is absent at –78 °C. Alkylation of **2as** with RMgCl (R = Me, Bz) or LiBz failed to provide the corresponding dialkyl complexes, with decomposition products always obtained.

All three isomers have been identified by NMR spectroscopy. Isomer **3as** is an asymmetric molecule that shows a NMR pattern similar to that described for isomer **2as**, containing eight resonances for the two C₅Me₄ groups, two for SiMe groups, two for the Cp ligands, and two for the new TiMe ligands, whereas the NMR spectra for either isomer **3aa** or **3ss** correspond to C₂ symmetry compounds, showing only four resonances for both C₅Me₄Si groups, one for both SiMe groups, one for both Cp ligands, and one for the new TiMe ligands. The relative disposition of the Me and Cp ligands with respect to the Si–O–Si bridge were identified by

(41) Buitrago, O.; de Arellano, C. R.; Jiménez, G.; Cuenca, T. *Organometallics* **2004**, *23*, 5873.

(42) Braunschweig, H.; Breitling, F. M.; Burschka, C.; Seeler, F. *J. Organomet. Chem.* **2006**, *691*, 702.

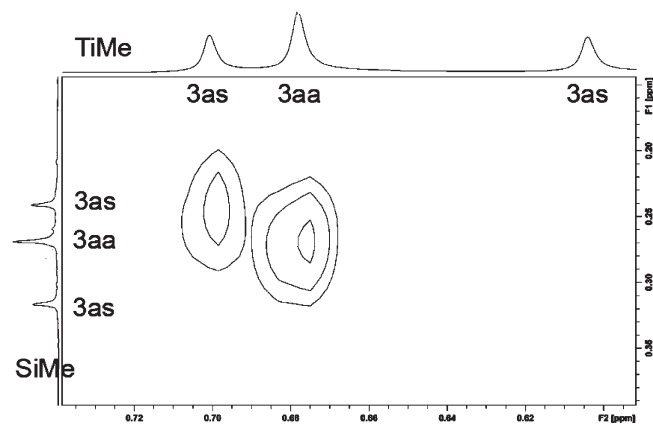


Figure 4. 2D NOE NMR spectrum of **3as** and **3aa** isomers showing interaction between TiMe ligands and SiMe groups.

NOE NMR experiments (Figure 4), which showed the Cp and Me ligands located in the *syn* position are closer to the SiMe group of the Ti–O–Si moiety to which they are bound. Finally, the reactivity of isomers **3** with Lewis acids described below is consistent with this assignment.

Formation of isomers **3aa** and **3ss** in the alkylation reaction of **2as** may result either from isomerization of the starting complex **2as** or from isomerization of the alkyl derivative **3as**, which is the expected product for this reaction, or alternatively from isomerization during the alkylation process. Several experiments have been realized in an attempt to determine how this isomerization occurs, employing solutions of complex **2as** and mixtures containing isomers **3as** and **3aa** obtained at -78 °C.

Thermal and photochemical isomerization^{43,44} of complexes **2as** and **3** was discounted after monitoring solutions of **2as** and **3** by NMR in the range between -60 and 80 °C and irradiating these solutions with visible and UV light. No modification was observed when the alkylation reaction was carried out in the presence or absence of visible light.

The influence of different ions present in solution (Li^+ , Cl^-) was also investigated.^{45–49} Addition of LiCl or $[\text{Bu}_4\text{N}]\text{Cl}$ to toluene and THF solutions of **2as** and **3** did not show any change in the range between -60 and 80 °C. However, addition of the lithium salt $\text{Li}[\text{B}(\text{C}_6\text{F}_5)_4]$, as a more soluble source of Li^+ , to **2as** gave a cationic compound, which will be described later. Conversely, no change was observed when $\text{Li}[\text{B}(\text{C}_6\text{F}_5)_4]$ was added to a THF solution of isomers **3as** and **3aa**, although decomposition occurred in toluene upon heating at 60 °C, contrasting with the thermal stability observed for these isomers.

These results suggest that isomerization occurred during the alkylation process. To clarify this proposal, theoretical calculations on the reaction mechanism were carried out by

considering that both Ti–Cl and Ti–O bonds of compound **2as** are susceptible to alkylation⁵⁰ (Scheme 3).

Stability of the Isomers of 2 and 3. In order to explain the different regioselectivity observed for the products of the reaction of **A** with 2 equiv of TiCp and the alkylation of **2as** with LiMe to form compounds **3**, we theoretically studied the relative stabilities of the three isomers of compounds **2** and **3**. The computational study requires calculating the energy of the optimized structures of the isomers of the series **2** and **3** (**as**, **aa**, and **ss**) in order to understand the stability trends. The calculated structural parameters of **2aa** are compared in Table 1 with those determined by X-ray diffraction for this compound. The good agreement found does support the methodology employed for the theoretical description of the systems. Of note is the concord found even in the nonbonding parameters, such as the $\text{Si}\cdots\text{Si}$ and $\text{Ti}\cdots\text{Ti}$ distances.

The relative energies in toluene of the calculated structures are gathered in Table 3. Isomer **2as** is considerably more stable than **2aa** and **2ss**. In contrast, the isomers of **3** have very similar energies. The relative energies in toluene of the isomers of **2** and **3** agree with the experimental trends: **2as** was obtained as the major ($>95\%$) or the unique product, whereas a mixture of the three possible isomers of **3** was found. To analyze the influence of the Cp ligand on the relative stabilities, we have calculated the isomers of a complex (**B**) derived from **2** by substituting the Cp ligand by a less bulky methyl group (Figure 5). In **B** the nomenclature **a-s** refers to the *anti* and *syn* position of Me with respect to Si–O–Si bridge. Results are very similar to those obtained for the **3** set, and a clearly favored isomer was not obtained. From these calculations it can be concluded that the regioselectivity is introduced by the combination of chloride and cyclopentadienyl ligands, vanishing when one of these ligands is changed for a methyl group.

Aiming to understand the origin of the preference for the **2as** isomer, we have carried out additional calculations in two series of compounds related to **2**. These compounds have the same coordination sphere as in **2** for the two titanium atoms, but the methyl groups attached to the $\text{C}_5\text{Me}_4\text{Si}$ ring (complexes **C**) or to the $\text{C}_5\text{Me}_4\text{Si}$ ligands and silicon atoms (complexes **D**) have been replaced by hydrogen atoms (Figure 5). Results for the **C** set (Table 3) show that the methyl substituents on the Cp ring have a very minor influence on the stability of the isomers. Isomer **Caa** remains at 2.8 kcal mol⁻¹ above the most stable **Cas**; the only change is a slight stabilization of **Css**, which lies 1.6 kcal mol⁻¹ above **Cas**. Thus, steric repulsions between methyl substituents on the $\text{C}_5\text{Me}_4\text{Si}$ ring and Si atom are partially responsible for the destabilization of **2ss**. It is interesting to note that, even at this level, without the methyl substituents, the energy trend describes greater stability for isomer **2as** with respect to **2aa** and **2ss**. Very similar results were obtained for complexes **D** (Table 3); **Daa** and **Dss** are found 3.6 and 1.2 kcal mol⁻¹ above the most stable **Das**. Removing the steric repulsion between methyl substituents on the silicon atom and the cyclopentadienyl ligands slightly stabilizes the *syn*–*syn* isomer, where this repulsion was more important (two methyl and Cp relatively close).

These calculations prove that the presence of methyl substituents on cyclopentadienyl and silicon is not the main influence responsible for regioselectivity in **2** isomers.

(43) Schmidt, K.; Reinmuth, A.; Rief, U.; Diebold, J.; Brintzinger, H. H. *Organometallics* **1997**, *16*, 1724.

(44) Collins, S.; Hong, Y. P.; Taylor, N. J. *Organometallics* **1990**, *9*, 2695.

(45) Buck, R. M.; Vinayavekhin, N.; Jordan, R. F. *J. Am. Chem. Soc.* **2007**, *129*, 3468.

(46) Curnow, O. J.; Fern, G. M.; Hamilton, M. L.; Zahl, A.; van Eldik, R. *Organometallics* **2004**, *23*, 906.

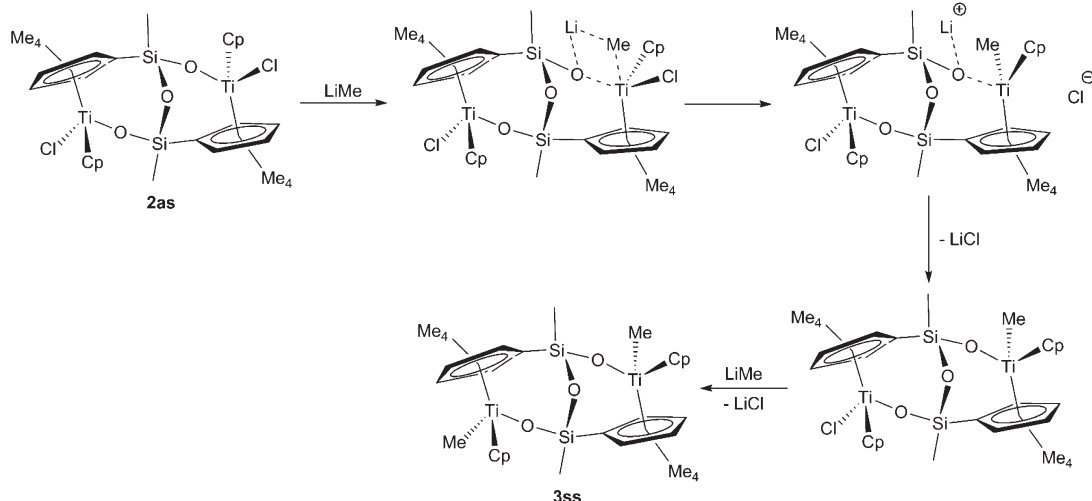
(47) Hollis, T. K.; Wang, L. S.; Tham, F. *J. Am. Chem. Soc.* **2000**, *122*, 11737.

(48) Yoder, J. C.; Day, M. W.; Bercaw, J. E. *Organometallics* **1998**, *17*, 4946.

(49) Meppelder, G. J. M.; Fan, H. T.; Spaniol, T. P.; Okuda, J. *Inorg. Chem.* **2009**, *48*, 7378.

(50) Nomura, K.; Naga, N.; Miki, M.; Yanagi, K.; Imai, A. *Organometallics* **1998**, *17*, 2152.

Scheme 3. Possible Alkylation Mechanism for Transformation of Isomer 2as into Isomer 3ss with Substitution of the Chloro Ligand Located at the *syn* Position^a



^aThe same process on the chloro ligand located at the *anti* positions would result in formation of isomer 3aa.

Table 3. Relative Energies in Toluene (ΔE^{tol} in kcal mol⁻¹) of the Optimized Structures of the Isomers of Compounds 2, 3, B, C, and D^a

isomer	ΔE^{tol}								
2as	0.0	3as	0.0	Bas	0.0	Cas	0.0	Das	0.0
2aa	3.1	3aa	0.1	Baa	0.1	Caa	2.8	Daa	3.6
2ss	3.1	3ss	0.2	Bss	0.6	Css	1.6	Dss	1.2

^aFor each series the energy of isomer as has been taken as a zero.

Repulsive interactions between cyclopentadienyl ligands and the Si–O–Si bridge can also be discarded from the different relative energies of parent compounds in series 2 and 3, despite the same disposition of cyclopentadienyl ligands in 2 and 3 related compounds. Moreover distances between the cyclopentadienyl ring centroid and the Si–O–Si bridging oxygen are long enough (between 5.4 Å for *syn*-cyclopentadienyl and 5.8 Å for *anti*-cyclopentadienyl) to preclude significant interactions.

The interligand angles reported in Table 1 for 2aa show significant deviations from a tetrahedral geometry. Hence, we have further explored this behavior optimizing the mononuclear titanium complexes E and F (Figure 6).

In Table 4 we have collected the angles describing the environment about titanium atoms in the mononuclear titanium complexes and in the as isomers of compounds 2, 3, and B. When only one cyclopentadienyl ring is present (E), the complex adopts the normal three-legged piano-stool geometry with the angles involving the Cp* (Cp* = C₅Me₅) ligand larger than those between the legs (115° and 103°, respectively). The presence of a second cyclopentadienyl ligand (F) markedly modifies the angles, with the two bulky cyclopentadienyl rings placed as far as possible apart (Cp*–Ti–Cp = 134°). In the bimetallic compounds analyzed, the strain caused by the presence of two bridges connecting the two Ti centers provokes notable changes in the angles, as can be appreciated by comparing the angles in F and 2as. In addition to the Cp*–Ti–Cp angles, the Cp*–Ti–O angles are also larger than 120°. When the Cp ligand is replaced by a methyl group in compound B, the C₅Me₄Si–Ti–O angle becomes the largest (about 130°), with the other angles approaching the usual tetrahedral values.

The presence of a methyl ligand allows a relaxation of the local geometry around the titanium centers, thus reducing the steric strain. Methyl is a ligand with electrons localized in the C–H bonds, whereas Cl and Cp ligands are electronically more cumbersome, having wide clouds of electrons diffusing all around and interacting with the electron clouds of the other ligands. In the case of series 3, the methyl groups are smaller than Cl, Me–Ti–L angles can be shorter, and so the substituents around Ti can be better accommodated, resulting in more relaxed geometries with similar energies. Substituting the chloride ligand of series 2 with the methyl of series 3, the ligands around Ti relax and the angles O–Ti–Cp and O–Ti–C₅Me₄Si increase, decreasing interligand repulsion and ring strain and, in this way, decreasing the energy difference between the compounds of the series. A detailed comparison of the coordination spheres around titanium atoms in compounds of series 2 and 3 and 2 and B is given in the Supporting Information.

Theoretical Study of 2 → 3 Isomerization. We have computationally examined the attack of methyl lithium on the two titanium centers of 2as. The reaction, carried out in toluene, yields three possible products, as shown previously in Scheme 2. Whereas the computational study of the stability of 2 and 3's isomers involved only geometry optimizations of minimum structures, in this case a complete exploration of the potential energy surface is needed, in order to locate transition states and determine reaction barriers. Given the dimensions of our system, a model system of the compound 2as was employed instead of the real system used above (Figure 7). We modeled complex 2as introducing the simplification of examining only one center at a time, with the hypothesis that the reaction on one center does not affect the other. This implies a sort of “commutativity” of attacks during the reaction (attacking Ti^a first and Ti^s in a second moment is the same as attacking Ti^s first and then Ti^a; from now on this will be implicitly assumed). Actually, given that the two Ti centers are far away from each other in 2as (5.376 Å), this can be considered quite a good approximation. Nevertheless, the attacks on the 2as Ti centers are quite different from each other and have to be studied separately; that is, each reaction center has to be simulated. In light of

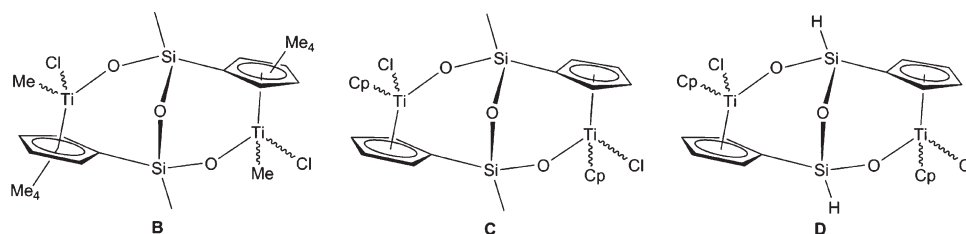


Figure 5. Structure drawing of modified complexes (**B**, **C**, **D**) designed for theoretical calculations.

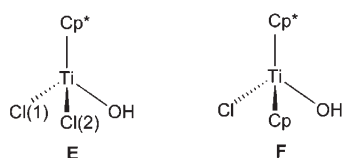


Figure 6. Structure drawing of mononuclear complexes (**E**, **F**) designed for theoretical calculations.

Table 4. Angles (deg) Describing the Environment of the Titanium Centers in the Calculated Mono- and Dinuclear Complexes^a

angle	E	F	2as	3as	Bas
	(X1 = Cl X2 = Cl)	(X1 = Cp X2 = Cl)	(X1 = Cp X2 = Cl)	(X1 = Cp X2 = Me)	(X1 = Me X2 = Cl)
Cp'-Ti-O	114.8	102.1	121.4/120.0	123.4/122.2	131.3/130.3
Cp'-Ti-X1	114.9	134.2	124.4/122.9	123.5/122.3	107.7/103.6
Cp'-Ti-X2	115.0	106.9	102.3/105.2	102.5/104.5	108.0/112.6
X1-Ti-O	103.4	107.5	104.6/104.6	106.1/105.5	99.2/99.8
X2-Ti-O	103.4	96.5	93.3/96.8	90.7/94.1	106.2/106.1
X1-Ti-X2	103.8	103.6	104.4/102.8	102.3/102.4	100.0/99.0

^a Cp' stands for Cp* (Cp* = C₅Me₅) in complexes **E** and **F** and for C₅Me₄Si in complexes **2**, **3**, and **B**.

the previous considerations, compound **2as** was simplified using two model systems, named **Gs** and **Ga**, differing in the *syn* and *anti* position of the Cp ligand with respect to the Si-O-Si bridge (Figure 7). In these models, the methyl groups on each C₅Me₄Si as well as the methyl substituent on the Si linked to the O-Ti have been considered. In addition, to keep the Si-O-Si bridge fixed, a CH₂-CH₂ chain has been added in order to simulate the rigidity of compound **2as**. However, the description of the organolithium reagent required some test calculations. Solvent effects are very important in organolithium chemistry, and they dramatically influence the aggregation state and reactivity of alkyllithium compounds.⁵¹⁻⁵⁸ Test calculations proved that only one molecule of toluene is coordinated to the lithium atom of LiMe. For this reason LiMe(tol) (**H**) was chosen as reagent (see Supporting Information for further discussion on the choice of the model system). Thus, the solvent (toluene) was considered in two ways in the compu-

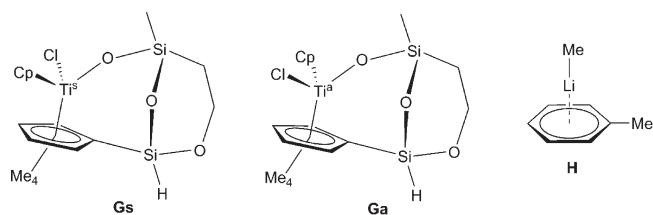


Figure 7. Model complexes and reagent considered in the theoretical study of the alkylation reaction.

Table 5. Relative Energies in Toluene (in kcal mol⁻¹) of the Six Different Possible Attacks Analyzed^a

attack	I	TS	F	[<i>d</i> (∞)] ^b	energy barrier	configuration
LiO(A)	-3.4	7.0	-1.7	-34.6	10.4	A→S
LiCl(A)	-3.9	17.4	-41.7	-34.6	21.3	A→A
LiOb(A)	-6.1	22.2	-18.9	-34.6	28.3	A→A
LiO(S)	-10.1	15.3	-26.3	-34.8	25.4	S→A
LiCl(S)	-5.2	13.4	-34.8	-34.8	18.6	S→S
LiOb(S)	-2.5	13.3	-11.7	-34.8	15.8	S→A

^a The letter in parentheses, in each attack, designates the center under attack. The energy of the reactants at infinite distance is taken as zero. Configuration refers to the change of the configuration of the Ti center; for example, A→S means that the reaction happens to a Ti⁴ center that changes its configuration, in the final product, to a Ti³. ^b The final product and LiCl(tol) at infinite distance.

tational study of the reaction: explicitly, by coordinating one molecule of toluene to LiMe, and implicitly by doing refinement calculations in a uniform dielectric solvent as before, using the CPCM model (solvent = toluene, $\epsilon = 2.379$).

Given the simplifications introduced in the system, due to computational limitations, and the subtle differences that could account for the temperature-dependent relative proportion of isomers, a quantitative agreement with the proportions of isomers of **3** obtained is beyond the scope of the investigation. The goal of the calculations is to assess the existence of low-energy pathways able to transform **2as** in the three isomers of **3** and to analyze the reaction mechanism for the alkylation of **2as** with LiMe. The reaction can be portrayed as the approach of a LiMe compound to one of the two Ti centers of **2as**, the donation of a Me⁻ anionic group, and the extraction of a Cl⁻ anionic group, with subsequent elimination of LiCl. In **2as** there are three basic centers available to anchor the lithium prior to methyl transfer: two oxygens and a chloride. We have considered the three possible approaches: (1) attack of **H** on the Ti center after a previous coordination to the oxygen atom bonded to C₅Me₄Si (*LiO*); (2) attack of **H** on the Ti center after a previous coordination of the Li⁺ cation to the Cl atom linked to Ti (*LiCl*); (3) attack of **H** on the Ti center after a previous coordination to the oxygen atom of the Si-O-Si bridge (*LiOb*; O_b = O₃; see Figure 3).

(51) Pratt, L. M.; Truhlar, D. G.; Cramer, C. J.; Kass, S. R.; Thompson, J. D.; Xidos, J. D. *J. Org. Chem.* **2007**, *72*, 2962.

(52) Pratt, L. M.; Ramachandran, B.; Xidos, J. D.; Cramer, C. J.; Truhlar, D. G. *J. Org. Chem.* **2002**, *67*, 7607.

(53) Leroy, B.; Marko, I. E. *J. Org. Chem.* **2002**, *67*, 8744.

(54) Katritzky, A. R.; Xu, Y.-J.; Jian, R. *J. Org. Chem.* **2002**, *67*, 8234.

(55) Mogali, S.; Darville, K.; Pratt, L. M. *J. Org. Chem.* **2001**, *66*, 2368.

(56) Streitwieser, A.; Juaristi, E.; Kim, Y.-J.; Pugh, J. *Org. Lett.* **2000**, *2*, 3739.

(57) Fraenkel, G.; Duncan, J. H.; Martin, K.; Wang, J. *J. Am. Chem. Soc.* **1999**, *121*, 10538.

(58) Hoffmann, D.; Collum, D. B. *J. Am. Chem. Soc.* **1998**, *120*, 5810.

Considering that each of these attacks can happen both to Ti^{a} and to Ti^{s} , we have six possible pathways. All of which have been explored. In each pathway an initial intermediate (**I**), a transition state describing the methyl transfer (**TS**), and a final intermediate (**F**) have been located. The relative energies of these structures in toluene, taking as a zero energy that of **Gs** (or **Ga**) together with **H** at infinite distance (for the attacks on the Ti^{s} and Ti^{a} centers, respectively), are collected in Table 5. Figure 8 shows the energy profiles. In Table 6

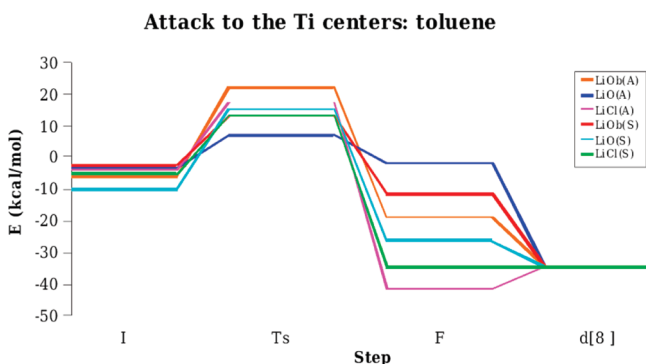


Figure 8. Plot of the different energies (as reported in Table 4) computed for the four steps of the six different attacks of $\text{LiMe}(\text{tol})$ to **Ga** and **Gs** in toluene.

more detailed information is reported about the changes in the most important distances describing the process: the $\text{Ti}-\text{Me}$ distance (the bond that is being formed), the $\text{Ti}-\text{Cl}$ and $\text{Li}-\text{Me}$ distances (the bonds that are being broken), and $\text{Li}-\text{X}$ ($\text{X} = \text{O}_b, \text{O},$ or Cl , according to the attack).

Important conclusions about the reaction mechanism can be deduced from these results. First, despite the similarity of Ti^{a} and Ti^{s} centers, differing only in the position of two substituents, each can sometimes react in a quite different way. Second, whereas several of the attacks take place with *retention of stereochemical configuration*, others happen with *inversion of stereochemical configuration*. This aspect is indicated in Table 5 as $\text{A} \rightarrow \text{S}$ or $\text{S} \rightarrow \text{A}$ (inversion) and $\text{A} \rightarrow \text{A}$ or $\text{S} \rightarrow \text{S}$ (retention). Calculations confirm that the formation of the three isomers of **3** in the alkylation reaction of **2as** is produced during the alkylation process.

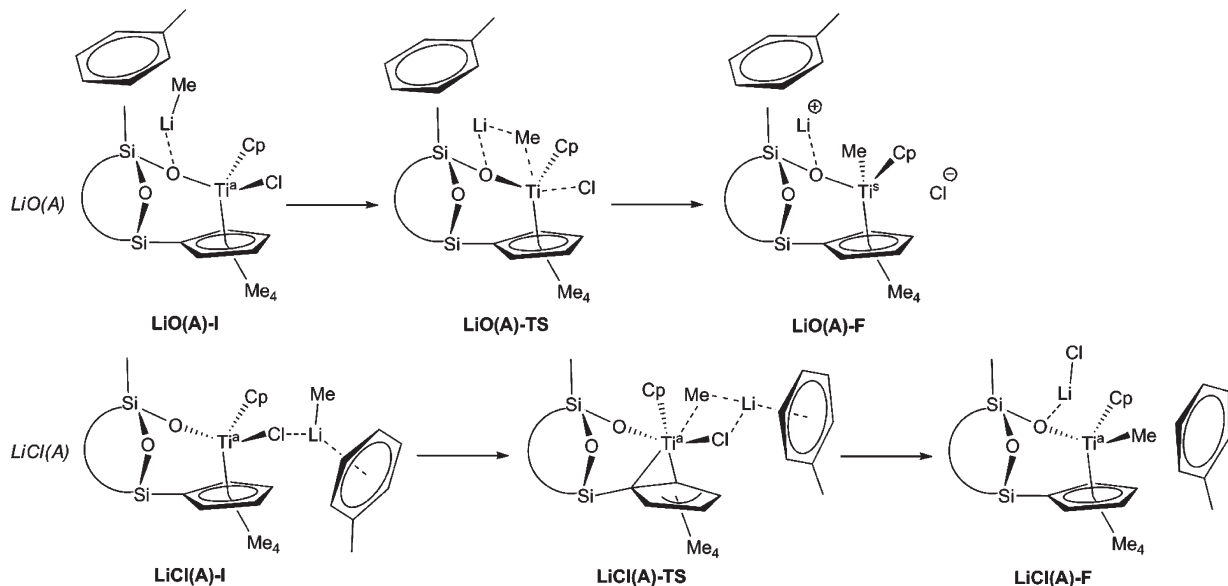
The lowest energy pathway for methylation of Ti^{a} of **2as** with retention of configuration (thus keeping a Ti^{a} stereochemistry in **3**) is the $\text{LiCl}(\text{A})$ attack, whereas the $\text{LiO}(\text{A})$ attack is the lowest with inversion of configuration. The main steps of these two attacks to Ti^{a} are depicted in Scheme 4. In the TS of the $\text{LiCl}(\text{A})$ pathway there is a slippage of the $\text{C}_5\text{Me}_4\text{Si}$ ring, which changes from an initial η^5 coordination to a η^2 coordination in this transition state. Accordingly, a rather high energy barrier is found for this step. In the $\text{LiO}(\text{A})$ pathway Me attacks on the opposite side

Table 6. Most Relevant Distances (\AA) in All the Attacks^a

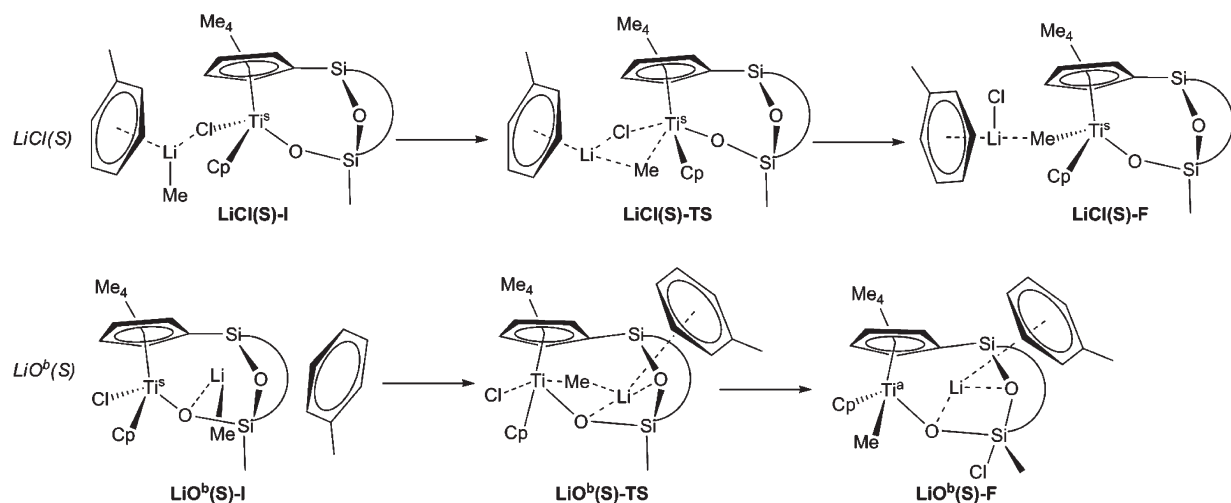
attack	$d_{\text{I}}(\text{Li}-\text{Me})/$ $d_{\text{TS}}(\text{Li}-\text{Me})/$ $d_{\text{F}}(\text{Li}-\text{Me})$	$d_{\text{I}}(\text{Ti}-\text{Me})/$ $d_{\text{TS}}(\text{Ti}-\text{Me})/$ $d_{\text{F}}(\text{Ti}-\text{Me})$	$d_{\text{I}}(\text{Li}-\text{X})/$ $d_{\text{TS}}(\text{Li}-\text{X})/$ $d_{\text{F}}(\text{Li}-\text{X})$	$d_{\text{I}}(\text{Ti}-\text{Cl})/$ $d_{\text{TS}}(\text{Ti}-\text{Cl})/$ $d_{\text{F}}(\text{Ti}-\text{Cl})$
$\text{LiO}(\text{A})$	2.011/2.003/2.177	4.795/3.157/2.303	1.900/1.784/1.755	2.365/2.569/2.821
$\text{LiCl}(\text{A})$	2.023/2.004/2.540	5.021/3.309/2.171	2.387/2.199/2.142	2.486/2.529/4.724
$\text{LiOb}(\text{A})$	2.010/2.009/3.251	7.687/3.189/2.150	1.956/1.935/1.898	2.389/2.520/5.326
$\text{LiO}(\text{S})$	2.033/1.991/2.498	5.026/3.313/2.169	1.990/1.786/1.733	2.429/2.470/2.352
$\text{LiCl}(\text{S})$	2.022/1.987/2.266	4.993/3.176/2.181	2.390/2.136/2.122	2.473/2.792/5.928
$\text{LiOb}(\text{S})$	1.997/2.010/2.255	4.884/3.148/2.216	3.493/2.131/1.863 1.912/1.903/1.932	2.360/2.564/4.334

^a d_{I} is the distance at the *I* geometry, d_{TS} is the distance measured at the transition state geometry, and d_{F} is the corresponding distance in the final intermediate. X corresponds either to $\text{O}_b, \text{O},$ or Cl , depending on the initial site of coordination of compound **H**.

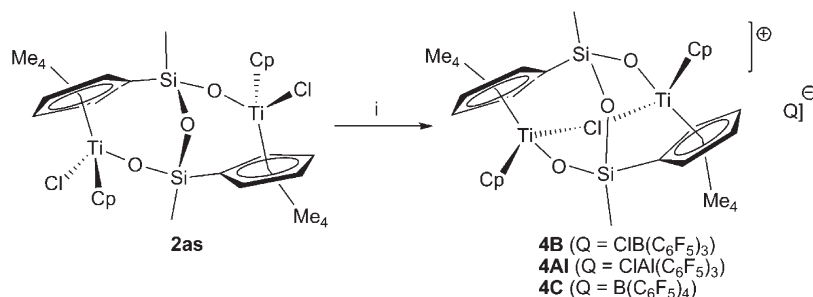
Scheme 4. Lowest Energy Pathway for Methylation of Ti^{a} of **2as** with Inversion of Configuration ($\text{LiO}(\text{A})$ attack, upper) and with Retention of Configuration ($\text{LiCl}(\text{A})$ attack, bottom)



Scheme 5. Lowest Energy Pathway for Methylation of Ti^s of **2as with Retention of Configuration ($LiCl(S)$ attack, upper) and with Inversion of Configuration ($LiO^b(S)$ attack, bottom)**



Scheme 6^a



^a (i) $E(C_6F_5)_3$ ($E = B, Al$) or $Li[B(C_6F_5)_4]$.

of the Cl atom (the angle $Me-Ti-Cl$ is about 150°), making this attack a sort of S_N2 reaction. The S_N2 character of the reaction entails a change in the configuration of the Ti center. The small change in geometry, going from the initial intermediate to the TS, is the cause of the lowest energy barrier of all six attacks studied. The $LiOb(A)$ happens with retention of configuration, but its transition state is quite high in energy, due to its stretched geometry (see Supporting Information).

The lowest energy pathways for methylation of Ti^s with retention and inversion of configuration are shown in Scheme 5. The $LiCl(S)$ attack is the lowest energy pathway for methylation of Ti^s of **2as** with retention of configuration (thus keeping a Ti^s stereochemistry in **3**), as the $LiCl(A)$ attack was for methylation of Ti^a of **2as** with retention of configuration. The transition state is basically an exchange of two groups (Me and Cl) between the reactant and the substrate. The fact that it does not involve strong distortions is the reason for its relatively low barrier. This attack is similar to $LiCl(A)$. $LiOb(S)$ is the lowest energy pathway for methylation of Ti^s of **2as** with inversion of configuration. Table 4 and Scheme 5 demonstrate how the approach should be more properly called $Li-O$ rather than $Li-O_b$, as in the initial state the Li atom is much closer to the oxygen atom bonded to Ti than to the oxygen atom of the $Si-O-Si$ bridge. During the transition state the Li atom coordinates to both available oxygen atoms (the O bonded to Ti and O_b) and starts a weak interaction with toluene. All these interactions make this transition state the second most stable

(after $LiO(A)$), and its activation energy is quite low. This double coordination is the reason that, in Table 5, two rows of numbers for the $Li-X$ value are reported. The first refers to the $Li-O_b$ distance, while the second refers to the $Li-O$ bond (where the oxygen atom is linked to Ti). As in the case of $LiO(A)$, given the opposite direction from which the Me ligand approaches the Ti center with respect to the Cl ligand, this can also be regarded as an S_N2 mechanism (angle $Me-Ti-Cl$ in TS 151.3°). The product is characterized by the migration of the Cl^- anion to the closest Si atom, creating a bipyramid whose center is the Si atom and the opposite vertices are O_b and Cl. This structure, quite high in energy, is more stable than those characterized by a separation of charges. This attack happens with *inversion of stereochemical configuration* ($S \rightarrow A$). The low activation barrier makes this attack the favorite to create a Ti^a center in **3** from a Ti^s in **2**. The $LiO(S)$ attack also entails inversion of configuration but has a notably higher energy barrier (see Supporting Information).

The three isomers of **3** can be obtained from **2as** by combining sequentially two attacks. Isomer **3as** can be formed by a $LiO(A)$ attack (which transforms a Ti^a center in **2as** into a Ti^s center in **3as**) followed by a $LiOb(S)$ attack (which transforms a Ti^s center in **2as** into a Ti^a center in **3as**), isomer **3aa** can be obtained by a $LiCl(A)$ attack and then $LiOb(S)$ attack, and finally, isomer **3ss** can be obtained by $LiO(A)$ and $LiCl(S)$ attacks. In the model systems considered (**Gs** and **Ga**), the highest energy barriers for such transformations are $15.8 \text{ kcal mol}^{-1}$ (**2as** \rightarrow **3as**), $21.3 \text{ kcal mol}^{-1}$

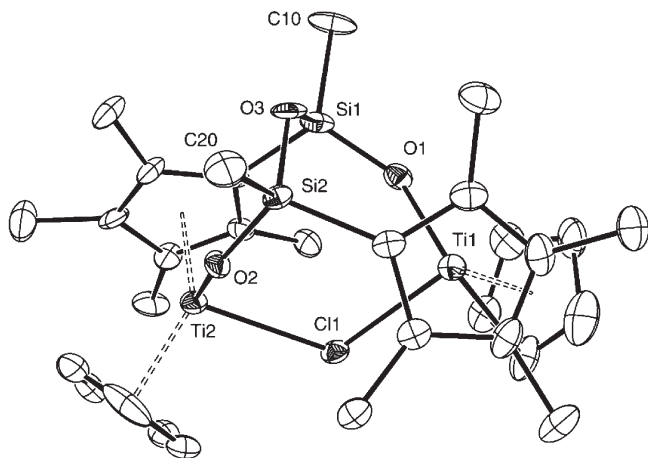


Figure 9. ORTEP plot of the molecular structure of cation $[(\text{TiCp})_2(\mu\text{-}\{\eta^5\text{-C}_5\text{Me}_4\text{SiMeO}\}_2(\mu\text{-O}))](\mu\text{-Cl})]^+$ (4^+) in the solid state. Thermal ellipsoids are drawn at the 30% probability level. Hydrogen atoms are omitted for clarity.

(**2as** \rightarrow **3aa**), and 18.6 kcal mol $^{-1}$ (**2as** \rightarrow **3ss**). Although these values cannot account for the proportion of isomers of **3** obtained experimentally, they do support the possible formation of the three isomers of **3** from the alkylation of **2as**.

Reactions of 2as with Lewis Acids. The dichloro compound **2as** reacted with the Lewis acids $\text{E}(\text{C}_6\text{F}_5)_3$ ($\text{E} = \text{B}, \text{Al}$) and the lithium salt $\text{Li}[\text{B}(\text{C}_6\text{F}_5)_4]$ to give the chloro-bridged compounds $[(\text{TiCp})_2(\mu\text{-}\{\eta^5\text{-C}_5\text{Me}_4\text{SiMeO}\}_2(\mu\text{-O}))](\mu\text{-Cl})[\text{Q}]$ (**4**; $\text{Q} = \text{ClB}(\text{C}_6\text{F}_5)_3$, **4B**; $\text{ClAl}(\text{C}_6\text{F}_5)_3$, **4Al**; $\text{Q} = \text{B}(\text{C}_6\text{F}_5)_4$, **4C**) (Scheme 6) as the only reaction products. The cation 4^+ is formed by abstraction of the chloro ligand located at the *syn* position, because only the chloro ligand in the *anti* position can close a bridge between both Ti atoms. Theoretical calculations indicate that 4^+ is the thermodynamic and kinetic product of the reaction (see below). The ^1H and ^{13}C NMR spectra are consistent with formation of these C_2 symmetry compounds, for which only four resonances for both C_5Me_4 ligands, one for both SiMe groups, and for both Cp ligands were observed. Furthermore, the ^{19}F NMR spectra of these species confirm the formation of the corresponding anions $[\text{ClB}(\text{C}_6\text{F}_5)_3]^-$, $[\text{ClAl}(\text{C}_6\text{F}_5)_3]^-$, and $[\text{B}(\text{C}_6\text{F}_5)_4]^-$. 19,59 An X-ray diffraction study for compound **4C** was carried out, confirming the proposed structure for this complex (Figure 9), 60,61 with a Cl atom bridging both Ti atoms.

Addition of excess $\text{E}(\text{C}_6\text{F}_5)_3$ ($\text{E} = \text{B}, \text{Al}$) or $\text{Li}[\text{B}(\text{C}_6\text{F}_5)_4]$ to complexes **2as** or 4^+ did not cause the abstraction of the second chloro ligand even in the presence of donor ligands

(59) Zhou, J.; Lancaster, S. J.; Walker, D. A.; Beck, S.; Thornton-Pett, M.; Bochmann, M. *J. Am. Chem. Soc.* **2001**, *123*, 223.

(60) Although many efforts have been done to obtain suitable crystals of **4C** for X-ray analysis, only crystals of poor quality have been so far obtained, so that although the identity of the complex was unambiguously established, the anion $\text{B}(\text{C}_6\text{F}_5)_4^-$ is very disordered and the distances and angles may not be very reliable.

(61) Crystal data for **4C**: $\text{C}_{54}\text{H}_{34}\text{ClB}_2\text{ClF}_{20}\text{O}_3\text{Si}_2\text{Ti}_2 \cdot (\text{C}_6\text{H}_6)$, $M_r = 1387.16$, crystal size $0.42 \times 0.32 \times 0.25$ mm 3 , monoclinic, space group $P2_1/c$, $a = 15.199(4)$ Å, $b = 18.274(5)$ Å, $c = 24.262(5)$ Å, $\beta = 90.60(3)^\circ$, $V = 6738(3)$ Å 3 , $Z = 4$, $\rho_{\text{calcd}} = 1.367$ mg m $^{-3}$, $\mu = 0.408$ mm $^{-1}$, Mo K α radiation ($\lambda = 0.71073$ Å). Data collection was performed at 200(2) K on a Nonius Kappa CCD single-crystal diffractometer. Reflections collected/unique 43 274/11 831. The final cycle of full matrix least-squares refinement based on 17 03 reflections and 827 parameters converged to final values of $R_1(F^2 > 2\sigma(F^2)) = 0.1765$, $wR_2(F^2 > 2\sigma(F^2)) = 0.4612$, $R_1(F^2) = 0.2085$, $wR_2(F^2) = 0.5007$. Largest diff peak/hole 2.686/1.007 e Å $^{-3}$.

Table 7. Distances (Å) between the Remaining Cl Atom (Cl^a for product **J** and Cl^s for product **K**) and the Ti Centers a

	$d(\text{Cl}-\text{Ti}^s)$	$d(\text{Cl}-\text{Ti}^a)$	ΔE
J	2.589	2.589	0.0
K	2.358	6.957	18.3

a Ti^s is the Ti linked to Cl^s (in compound **2as**), and Ti^a is the Ti linked to Cl^a (in **2as**). Energies were obtained in toluene, and ΔE (kcal mol $^{-1}$) refers to the difference in energy with product **J**.

such as py or thf. Moreover, addition of these donor ligands to solutions of **4B** and **4Al** selectively regenerates the starting complex **2as** with formation of adducts $\text{L} \cdot \text{E}(\text{C}_6\text{F}_5)_3$.

Theoretical Study of Chloride Abstraction. The experimental study shows that during the electrophilic attack of compounds of the type $\text{E}(\text{C}_6\text{F}_5)_3$ ($\text{E} = \text{B}, \text{Al}$) and $\text{Li}[\text{B}(\text{C}_6\text{F}_5)_4]$ to the dichloro compound **2as** only one of the two Cl ligands is lost, forming cation 4^+ . In order to evaluate possible differences between both chloride ligands in **2as**, we performed a natural bond orbitals (NBO) analysis of the stabilization energy due to orbital interactions for both chlorides. 62,63 Overall, the summation of all the contributions to the stabilization of the chloro ligands of compound **2as** points out a small difference between Cl^s and Cl^a (see Supporting Information). The stabilization of Cl^a to the **2as** compound is 4.4 kcal mol $^{-1}$ greater than that of Cl^s , suggesting that its removal would destabilize the molecule more than losing Cl^s . The analysis of the stability of the two different products once a chloride has been removed gives the reason for the preferred abstraction of the chloro ligand located at the *syn* position. The relative energies of the two possible products obtained by optimization after the removal of one chloride are collected in Table 7 (DFT/BS1 calculations). Product **J** is obtained from **2as** removing Cl^s (in *syn* position with respect to Si–O–Si), while product **K** is obtained from **2as** removing Cl^a (in *anti* position).

From the distances collected in Tables 7 an important difference between **J** and **K** products can be noticed. Whereas in product **K** the removal of Cl^a causes a small local rearrangement of the Ti^a ligands, but leaves the other part of the molecule (the one with Cl^s) basically unchanged, the removal of the Cl^s atom in product **J** causes a huge rearrangement of the geometry of the whole molecule, ending with the Cl^a atom bridging between the two Ti centers, as evidenced by the distances between the remaining chlorine and the Ti centers. The structure of **J** agrees with the X-ray determined structure of 4^+ . The rearrangement of the Cl^a atom, bridging between the two Ti centers, stabilizes the molecule by about 20 kcal mol $^{-1}$ with respect to product **K**. In this way, the dissociation of the Cl^s atom is thermodynamically preferred. This fact, combined with the easier extraction of the Cl^s atom, makes this chloro ligand the better candidate for an electrophilic reaction, as proved by experiments.

Reactions of 3 with Lewis Acids. As discussed above, methylation of **2as** under different thermal conditions always afforded mixtures containing variable amounts of the three possible isomers of the dimethyl compound **3**, from which none could be isolated as a pure component. Therefore,

(62) Weinhold, F.; Landis, C., *Valency and Bonding. A Natural Bond Orbital Donor-Acceptor Perspective*; Cambridge University Press: Cambridge, U.K., 2005.

(63) Reed, A. E.; Curtiss, L. A.; Weinhold, F. *Chem. Rev.* **1988**, *88*, 899.

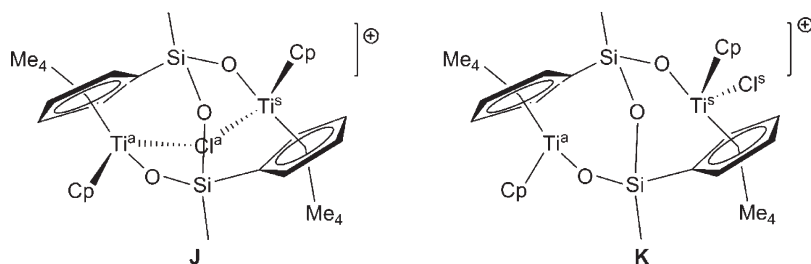
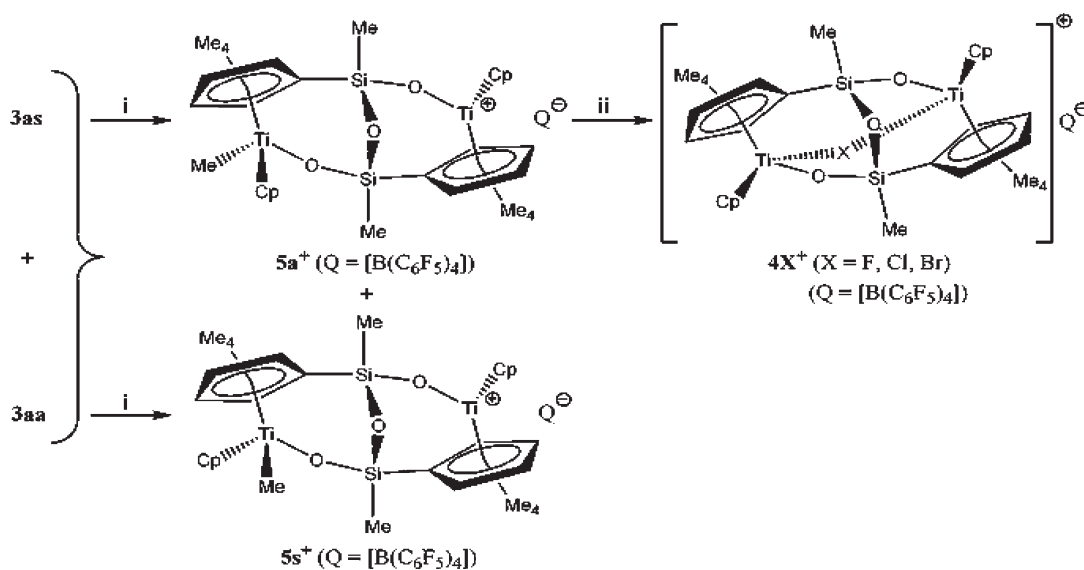


Figure 10. Structure drawing of mononuclear complexes (J, K) designed for theoretical calculations.

Scheme 7^a



^a(i) $[\text{Ph}_3\text{C}][\text{B}(\text{C}_6\text{F}_5)_4]$, $-70\text{ }^\circ\text{C}$; (ii) XC_6D_5 ($\text{X} = \text{F}, \text{Cl}, \text{Br}$) or CD_2Cl_2 , rt.

studies of their reactivity with Lewis acids with the aim of generating cationic complexes had to be carried out using mixtures of isomers. We have focused our studies on the products obtained at $-78\text{ }^\circ\text{C}$ (see Table 4), with a **3as**:**3aa** molar ratio of 1:1 due to the lack of purity of mixtures obtained at higher temperatures. It is important to note that isomer **3as** shows two different methyl groups located at *syn* and *anti* positions, respectively, whereas both methyl groups of isomer **3aa** are located at *syn* positions.

Reactions with the Lewis acids $\text{E}(\text{C}_6\text{F}_5)_3$ ($\text{E} = \text{B}, \text{Al}$) of the equimolar mixture of **3as** and **3aa** unfortunately failed to give any identifiable product even at low temperature. However, addition of $[\text{Ph}_3\text{C}][\text{B}(\text{C}_6\text{F}_5)_4]$ to a CD_2Cl_2 solution of **3as** and **3aa** at $-70\text{ }^\circ\text{C}$ gave a mixture containing a 1:1 molar ratio of two isomers $[(\text{TiCpMe})(\text{TiCp})(\mu\text{-}\{\eta^5\text{-C}_5\text{Me}_4\text{SiMeO}\}_2(\mu\text{-O}))]^+$ (**5a⁺** and **5s⁺**), which resulted from the abstraction of one of the methyl groups to leave the remaining methyl ligand at *anti* and *syn* positions, respectively (Scheme 7).

The 1:1 molar ratio of the resulting mixture of isomers corresponds exactly with the initial molar ratio of **3as**:**3aa**, demonstrating that **5s⁺** was formed from **3aa** only and not from **3as**. Consequently, methyl abstraction from **3as** must be *regiospecific*, as only the methyl group located at the *syn* position of the two different methyl groups present can be abstracted; this is the same behavior observed for the reaction of **2as** with Lewis acids.

The ^1H and ^{13}C NMR spectra of this mixture are consistent with the presence of two compounds that are asymmetric molecules and show eight resonances for two $\text{C}_5\text{Me}_4\text{Si}$

rings, two resonances for both SiMe groups and two for both Cp ligands, and finally one resonance for the remaining TiMe group for each isomer.

When the temperature was increased, isomer **5a⁺** was transformed into the chloro-bridged cationic complex **4⁺**, and after several hours at room temperature isomer **5s⁺**, which cannot be transformed into the bridging species, was completely decomposed. The same behavior was observed when XC_6D_5 ($\text{X} = \text{F}, \text{Cl}, \text{Br}$) was employed as solvent, affording the respective cationic compounds $[(\text{TiCp})_2(\mu\text{-}\{\eta^5\text{-C}_5\text{Me}_4\text{SiMeO}\}_2(\mu\text{-O}))(\mu\text{-X})]^+$ ($\text{X} = \text{F}$, **4F⁺**; Cl , **4Cl⁺**; Br , **4Br⁺**) at room temperature, which showed very similar ^1H and ^{13}C NMR spectra. The ^{19}F NMR spectrum of the **4F⁺** cation showed a broad resonance at negative values ($\delta = -53.3$), corresponding to the Ti–F–Ti bridge.^{19,64}

Finally, as we have reported previously with other dinuclear complexes of this type, addition of an excess of any Lewis acid, $\text{E}(\text{C}_6\text{F}_5)_3$ ($\text{E} = \text{B}, \text{Al}$) or $[\text{Ph}_3\text{C}][\text{B}(\text{C}_6\text{F}_5)_4]$, did not afford dicationic complexes, even in the presence of donor ligands.^{37,38}

Conclusions

The introduction of only one Cp ligand in the dinuclear compound $[(\text{TiCl}_2)_2(\mu\text{-}\{\eta^5\text{-C}_5\text{Me}_4\text{SiMeO}\}_2(\mu\text{-O}))]$ (**A**), with two different chloro ligands on each Ti atom with

(64) Perdih, F.; Pevec, A.; Petricek, S.; Petric, A.; Lah, N.; Kogej, K.; Demsar, A. *Inorg. Chem.* **2006**, *45*, 7915.

respect to the Si–O–Si bridge, is more favorable in one of the two possible positions, although a mixture of both possible isomers of $[(\text{TiClCp})(\text{TiCl}_2)(\mu\text{-}\{\eta^5\text{-C}_5\text{Me}_4\text{SiMeO}\}_2(\mu\text{-O}))]$ were obtained in the reaction of **A** with 1 equiv of TiCp at 80 °C. However addition of 2 equiv of TiCp at 80 °C to compound **A** gave the disubstituted isomer $[(\text{TiCpCl})_2(\mu\text{-}\{\eta^5\text{-C}_5\text{Me}_4\text{SiMeO}\}_2(\mu\text{-O}))]$ (**2as**) regioselectively, with each Cp ligand in *anti*–*syn* positions. According to the DFT studies, this is the lowest energy isomer of the three possible isomers that this reaction could produce. The isomer **2aa**, with both Cp ligands located at *anti* positions with respect to the Si–O–Si bridge, was also obtained as a minor product when the same reaction was carried out at 60 °C.

Reaction of isomer $[(\text{TiCpCl})_2(\mu\text{-}\{\eta^5\text{-C}_5\text{Me}_4\text{SiMeO}\}_2(\mu\text{-O}))]$ (**2as**) with LiMe in toluene gave the three possible isomers of $[(\text{TiCpMe})_2(\mu\text{-}\{\eta^5\text{-C}_5\text{Me}_4\text{SiMeO}\}_2(\mu\text{-O}))]$ (**3as**, **3ss**, **3aa**). The relative proportion of isomers was dependent on the reaction temperature, the total yield and purity being higher at –78 °C. A DFT study of the reaction mechanism shows that despite the similarity of Ti^{a} and Ti^{s} centers, each can sometimes react in a quite different ways. Moreover, the attack of LiMe can take place both with *retention of stereochemical configuration* and with *inversion of stereochemical configuration*. Calculations do confirm that the formation of the three isomers of **3** takes place during the alkylation process of **2as**.

Compound **2as** reacts with $\text{E}(\text{C}_6\text{F}_5)_3$ (E = B, Al) or $\text{Li}[\text{B}(\text{C}_6\text{F}_5)_4]$ to give the cationic chloro-bridged complex $[(\text{TiCp})_2(\mu\text{-}\{\eta^5\text{-C}_5\text{Me}_4\text{SiMeO}\}_2(\mu\text{-O}))(\mu\text{-Cl})]^+$ (**4⁺**) by abstraction of the Cl atom next to the Si–O–Si bridge. Formation of complex **4⁺** corresponds with the thermodynamic product of the reaction.

A mixture of isomers **3as** and **3aa** reacted with $[\text{Ph}_3\text{C}][\text{B}(\text{C}_6\text{F}_5)_4]$ to give a mixture of the cationic complexes $[(\text{TiCpMe})(\text{TiCp})(\mu\text{-}\{\eta^5\text{-C}_5\text{Me}_4\text{SiMeO}\}_2(\mu\text{-O}))]^+$ (**5a⁺** and **5s⁺**). Formation of **5a⁺** corresponds to the selective abstraction of the methyl group at the *syn* position with respect to the Si–O–Si bridge of isomer **3as**, whereas formation of complex **5s⁺** occurs only with abstraction of the methyl group *syn* to the Si–O–Si bridge of isomer **3aa**. Thus, the molar ratio **5a⁺**:**5s⁺** is the same as the initial molar ratio of **3as**:**3aa**. Complex **5a⁺** evolved at ambient temperature to the halogen-bridged complexes $[(\text{TiCp})_2(\mu\text{-}\{\eta^5\text{-C}_5\text{Me}_4\text{SiMeO}\}_2(\mu\text{-O}))(\mu\text{-X})]^+$ (X = F, Cl, Br) by methyl-halide exchange with the solvent (XC_6D_5 , X = F, Cl, Br; CD_2Cl_2).

Experimental Section

General Considerations. All manipulations were carried out under an argon atmosphere, and solvents were purified from appropriate drying agents. NMR spectra were recorded at 400.13 (¹H), 376.70 (¹⁹F), and 100.60 (¹³C) MHz on a Bruker AV400. Chemical shifts (δ) are given in ppm. ¹H and ¹³C resonances were measured relative to solvent peaks considering TMS = 0 ppm, while ¹⁹F resonances were measured relative to external CFCl_3 . Assignment of resonances was made from HSQC, HMBC, and NOESY NMR experiments. Elemental analyses were performed on a Perkin-Elmer 240C. Compounds $[(\text{TiCl}_2)_2(\mu\text{-}\{\eta^5\text{-C}_5\text{Me}_4\text{SiMeO}\}_2(\mu\text{-O}))]$ (**A**),³⁷ $\text{B}(\text{C}_6\text{F}_5)_3$,⁶⁵

$0.5(\text{toluene})\cdot\text{Al}(\text{C}_6\text{F}_5)_3$,⁶⁶ and $[\text{Ph}_3\text{C}][\text{B}(\text{C}_6\text{F}_5)_4]$ ⁶⁷ were prepared by literature methods. TiCp and $\text{Li}[\text{B}(\text{C}_6\text{F}_5)_4]$ were obtained from commercial sources.

$[(\text{TiCl}_2)_2(\mu\text{-}\{\eta^5\text{-C}_5\text{Me}_4\text{SiMeO}\}_2(\mu\text{-O}))]$ (**1**). A suspension of $[(\text{TiCl}_2)_2(\mu\text{-}\{\eta^5\text{-C}_5\text{Me}_4\text{SiMeO}\}_2(\mu\text{-O}))]$ (**A**) (0.20 g, 0.32 mmol) and TiCp (0.10 g, 0.38 mmol) in toluene (20 mL) was heated at 80 °C for 48 h. A 10 mL amount of hexane was then added, and the solution was filtered. The volatiles were pumped off to give a mixture of the two monosubstituted isomers (50% of major isomer (**1M**) by ¹H NMR and 17% of minor isomer (**1m**) by ¹H NMR), the disubstituted product **2as** (8% by ¹H NMR), and the starting material **A** (25% by ¹H NMR). ¹H NMR (C_6D_6): 0.29 (s, 3 H, SiMe, **1m**), 0.33 (s, 3 H, SiMe, **1m**), 0.34 (s, 3 H, SiMe, **1M**), 0.48 (s, 3 H, SiMe, **1M**), 1.45 (s, 3 H, C₅Me₄, **1M**), 1.58 (s, 3 H, C₅Me₄, **1m**), 1.60 (s, 3 H, C₅Me₄, **1M**), 1.95 (s, 3 H, C₅Me₄, **1m**), 2.03 (s, 3 H, C₅Me₄, **1M**), 2.08 (s, 3 H, C₅Me₄, **1M**), 2.10 (s, 3 H, C₅Me₄, **1m**), 2.11 (s, 3 H, C₅Me₄, **1M**), 2.15 (s, 3 H, C₅Me₄, **1m**), 2.18 (s, 3 H, C₅Me₄, **1M**), 2.20 (s, 3 H, C₅Me₄, **1M**), 2.20 (s, 3 H, C₅Me₄, **1m**), 2.37 (s, 3 H, C₅Me₄, **1M**), 2.42 (s, 3 H, C₅Me₄, **1m**), 2.48 (s, 3 H, C₅Me₄, **1M**), 2.58 (s, 3 H, C₅Me₄, **1m**), 5.90 (s, 5 H, C₅H₅, **1m**), 6.07 (s, 5 H, C₅H₅, **1M**). ¹³C NMR (C_6D_6): –3.2 and –1.5 (SiMe, **1m**), –2.1 and –2.4 (SiMe, **1m**), 11.9–15.4 (C₅Me₄, **1M** and **1m**), 119.0 (C₅H₅, **1m**), 120.1 (C₅H₅, **1M**), 119.2–148.3 (C₅Me₄, **1M** and **1m**).

$[(\text{Ti}(\eta^5\text{-C}_5\text{H}_5)\text{Cl})_2(\mu\text{-}\{\eta^5\text{-C}_5\text{Me}_4\text{SiMeO}\}_2(\mu\text{-O}))]$ (**2as**). A suspension of $[(\text{TiCl}_2)_2(\mu\text{-}\{\eta^5\text{-C}_5\text{Me}_4\text{SiMeO}\}_2(\mu\text{-O}))]$ (**A**) (0.90 g, 1.47 mmol) and TiCp (1.23 g, 4.41 mmol) in toluene (50 mL) was heated at 80 °C for 48 h, when 20 mL of hexane was added and the solution was filtered. The red residue was extracted again into a mixture of solvents toluene/hexane (30 mL/20 mL). The volatiles were removed under vacuum, leaving a red solid (0.88 g, 90%). ¹H NMR (CDCl_3): 0.11 (s, 3 H, SiMe), 0.18 (s, 3 H, SiMe), 1.62 (s, 3 H, C₅Me₄), 1.69 (s, 3 H, C₅Me₄), 2.16 (s, 3 H, C₅Me₄), 2.22 (s, 3 H, C₅Me₄), 2.23 (s, 3 H, C₅Me₄), 2.31 (s, 3 H, C₅Me₄), 2.33 (s, 3 H, C₅Me₄), 2.40 (s, 3 H, C₅Me₄), 6.05 (s, 5 H, C₅H₅), 6.26 (s, 5 H, C₅H₅). ¹³C NMR (CDCl_3): –1.7 and –0.1 (SiMe), 11.9, 12.8, 13.8, 14.3, 14.4, 15.2, 15.6, and 16.4 (C₅Me₄), 118.4 and 119.0 (C₅H₅), 119.1, 120.0, 122.4, 124.9, 127.0, 127.6, 131.9, 132.1, 139.0, and 147.1 (C₅Me₄). Anal. Calcd for $\text{C}_{30}\text{H}_{40}\text{O}_3\text{Si}_2\text{Ti}_2\text{Cl}_2$ (670.55): C, 53.69; H, 5.96. Found: C, 53.53; H, 5.84.

$[(\text{Ti}(\eta^5\text{-C}_5\text{H}_5)\text{Cl})_2(\mu\text{-}\{\eta^5\text{-C}_5\text{Me}_4\text{SiMeO}\}_2(\mu\text{-O}))]$ (mixture of **2aa** and **2as**). A suspension of $[(\text{TiCl}_2)_2(\mu\text{-}\{\eta^5\text{-C}_5\text{Me}_4\text{SiMeO}\}_2(\mu\text{-O}))]$ (**A**) (0.45 g, 0.73 mmol) and TiCp (0.91 g, 3.31 mmol) in toluene (50 mL) was heated at 60 °C for 48 h. After addition of hexane (20 mL), the solution was filtered. The remaining solution was cooled to –40 °C to give a mixture of the isomer **2as** (95%) and **2aa** (5%) (total yield 0.40 g, 87%). ¹H NMR (CDCl_3): 0.14 (s, 6 H, SiMe), 2.15 (s, 6 H, C₅Me₄), 2.24 (s, 6 H, C₅Me₄), 2.31 (s, 6 H, C₅Me₄), 2.33 (s, 6 H, C₅Me₄), 6.12 (s, 10 H, C₅H₅).

$[(\text{Ti}(\eta^5\text{-C}_5\text{H}_5)\text{Me})_2(\mu\text{-}\{\eta^5\text{-C}_5\text{Me}_4\text{SiMeO}\}_2(\mu\text{-O}))]$ (**3**). A solution of **2as** (0.30 g, 0.44 mmol) in toluene (30 mL) was treated with 2 equiv of LiMe (0.60 mL, 0.90 mmol) at the reaction temperature. After the corresponding reaction time, hexane (10 mL) was added and the whole filtered. The volatiles were removed under vacuum, yielding a mixture of the isomers **3as**, **3aa**, and **3ss** in different proportions depending on the temperature of the reaction (see Table 2). The yield decreases with increasing temperature, and the elemental analysis reported corresponds to the sample synthesized at –78 °C. Data for **3as**: ¹H NMR (C_6D_6): 0.24 (s, 3 H, SiMe), 0.31 (s, 3 H, SiMe), 0.60 (s, 3 H, TiMe), 0.70 (s, 3 H, TiMe), 1.20 (s, 3 H, C₅Me₄), 1.27 (s, 3 H, C₅Me₄), 1.56 (s, 3 H, C₅Me₄), 1.57 (s, 3 H, C₅Me₄), 2.10 (s, 3 H, C₅Me₄), 2.13 (s, 3 H, C₅Me₄), 2.30 (s, 3 H, C₅Me₄), 2.39 (s, 3 H, C₅Me₄), 5.69 (s, 5 H, C₅H₅), 5.84 (s, 5 H, C₅H₅). ¹³C (C_6D_6): 0.6 and 1.4 (SiMe), 40.3 and 43.6 (TiMe), 10.7, 10.9, 12.7, 12.8, 13.4, 14.1, 14.4, and 14.9 (C₅Me₄), 114.1 and 114.4 (C₅H₅), 117.1–135.5 (C₅Me₄). Data for **3ss**: ¹H NMR (C_6D_6): 0.27 (s, 6 H, SiMe), 0.68 (s, 6 H, TiMe), 1.63 (s, 6 H, C₅Me₄), 1.99

(65) Lancaster, S. In <http://www.syntheticpages.org/pages/215>, 2003, p 215.

(66) Feng, S. G.; Roof, G. R.; Chen, E. Y. X. *Organometallics* 2002, 21, 832.

(67) Lancaster, S. In <http://www.syntheticpages.org/pages/216>, 2003, p 216.

(s, 6 H, C_5Me_4), 2.00 (s, 6 H, C_5Me_4), 2.26 (s, 6 H, C_5Me_4), 5.76 (s, 10 H, C_5H_5). ^{13}C NMR (C_6D_6): -0.6 (SiMe), 41.8 (TiMe), 10.6, 12.8, 14.2, and 15.3 (C_5Me_4), 114.5 (C_5H_5), 117.1–135.5 (C_5Me_4). Data for **3aa**: 1H NMR (C_6D_6): 0.30 (s, 6 H, SiMe), 0.74 (s, 6 H, TiMe), 1.25 (s, 6 H, C_5Me_4), 1.52 (s, 6 H, C_5Me_4), 2.15 (s, 6 H, C_5Me_4), 2.22 (s, 6 H, C_5Me_4), 5.70 (s, 10 H, C_5H_5). Anal. Calcd for $C_{32}H_{46}O_3Si_2Ti_2$ (629.55): C, 60.99; H, 7.30. Found: C, 60.79; H, 7.14.

$\{[Ti(\eta^5-C_5H_5)_2(\mu-Cl)(\mu-\{(\eta^5-C_5Me_4SiMeO)_2(\mu-O)\})][Q](Q = CIB(C_6F_5)_3, 4B, Q = ClAl(C_6F_5)_3, 4A)\}$. Compounds **2as** (0.10 g, 0.15 mmol) and $E(C_6F_5)_3$ ($B(C_6F_5)_3$ 0.076 g, 0.15 mmol; (0.5 C_7H_8) \cdot Al(C_6F_5) $_3$ 0.085 g, 0.15 mmol) were stirred in CH_2Cl_2 (2 mL) for 5 min. The volatiles were removed under vacuum, and the oil was washed with hexane (2 mL) to give **4B** (0.150 g, 85%) and **4A** (0.152 g, 85%) as a brownish oils. Anal. Calcd for $C_{48}H_{40}O_3Si_2Ti_2F_{15}AlCl_2$ (1198.42): C, 48.06; H, 3.33. Found: C, 48.85; H, 3.80. Data for **4B**: 1H NMR ($CDCl_3$): 0.30 (s, 6 H, SiMe), 2.06 (s, 6 H, C_5Me_4), 2.12 (s, 6 H, C_5Me_4), 2.18 (s, 6 H, C_5Me_4), 2.50 (s, 6 H, C_5Me_4), 6.22 (s, 10 H, C_5H_5). ^{13}C NMR ($CDCl_3$): -0.1 (SiMe), 12.5, 13.8, 16.1, and 16.6 (C_5Me_4), 118.5, 120.5, 131.1, 141.2, and 145.8 (C_5Me_4), 121.3 (C_5H_5), 137.7 and 148.8 (m, C_6F_5). ^{19}F NMR ($CDCl_3$): -129.8 (o- C_6F_5), -163.5 (bs, m- C_6F_5 and p- C_6F_5). Data for **4A**: 1H NMR ($CDCl_3$): 0.30 (s, 6 H, SiMe), 2.06 (s, 6 H, C_5Me_4), 2.12 (s, 6 H, C_5Me_4), 2.18 (s, 6 H, C_5Me_4), 2.50 (s, 6 H, C_5Me_4), 6.22 (s, 10 H, C_5H_5). ^{13}C NMR ($CDCl_3$): -0.1 (SiMe), 12.5, 13.8, 16.1, and 16.6 (C_5Me_4), 118.5, 120.5, 131.1, 141.2, and 145.8 (C_5Me_4), 121.3 (C_5H_5), 136.6, 141.3, and 150.1 (m, C_6F_5). ^{19}F NMR ($CDCl_3$): -122.1 (o- C_6F_5), -156.5 (p- C_6F_5) and -163.2 (m- C_6F_5).

$\{[Ti(\eta^5-C_5H_5)_2(\mu-Cl)(\mu-\{(\eta^5-C_5Me_4SiMeO)_2(\mu-O)\})][B(C_6F_5)_4]$ (**4C**). Compounds **2as** (0.10 g, 0.15 mmol) and $LiB(C_6F_5)_4 \cdot 2.5C_4H_{10}O$ (0.13 g, 0.15 mmol) were stirred in toluene (2 mL) for 5 min. The solution was filtered, and the remaining solid was washed with hexane (2 \times 2 mL) to give the compound **4-C** (0.152 g, 0.12 mmol, 85%). 1H NMR ($CDCl_3$): 0.35 (s, 6 H, SiMe), 2.14 (s, 6 H, C_5Me_4), 2.16 (s, 6 H, C_5Me_4), 2.37 (s, 6 H, C_5Me_4), 2.38 (s, 6 H, C_5Me_4), 6.17 (s, 10 H, C_5H_5). ^{13}C NMR ($CDCl_3$): 0.3 (SiMe), 13.0, 13.3, 16.0, and 16.5 (C_5Me_4), 119.7, 133.6, 140.1, 143.2, and 149.7 (C_5Me_4), 120.1 (C_5H_5), 136.8, 139.7, and 149.4 (m, C_6F_5). ^{19}F NMR ($CDCl_3$): -133.5 (o- C_6F_5), -162.5 (p- C_6F_5) and -166.4 (m- C_6F_5). Anal. Calcd for $C_{54}H_{40}O_3Si_2Ti_2F_{20}BCl$ (1313.86): C, 49.32; H, 3.04. Found: C, 49.16; H, 3.11.

$\{[Ti(\eta^5-C_5H_5)_2(\mu-X)(\mu-\{(\eta^5-C_5Me_4SiMeO)_2(\mu-O)\})][B(C_6F_5)_4]$ (**5aC**, **5sC**). A 0.5 mL sample of CD_2Cl_2 previously cooled at $-78^\circ C$ was added to a mixture of **3as** and **3aa** in ca. 1:1 (0.015 g, 0.023 mmol) and 1 equiv of $[Ph_3C][B(C_6F_5)_4]$ (0.021 g, 0.023 mmol) in a NMR tube at $-78^\circ C$. The reaction was immediately monitored by NMR spectroscopy, showing a complete transformation into a mixture of **5aC**, **5sC**, and **4C** in ca. 1:2:1 after 5 min at $-50^\circ C$. The isomer **5a** $^+$ evolved to the chloro-bridged ionic compound **4** $^+$ at ambient temperature. Data for **5aC**: 1H NMR (CD_2Cl_2): 0.14 (s, 3 H, SiMe), 0.33 (s, 3 H, SiMe), 0.69 (s, 3 H, TiMe), 1.40–2.50 (s, 8 \times 3 H, C_5Me_4), 5.98 (s, 5 H, C_5H_5), 6.15 (s, 5 H, C_5H_5). ^{13}C NMR (CD_2Cl_2): 53.4 (TiMe). ^{19}F NMR (CD_2Cl_2): -133.5 (o- C_6F_5), -162.5 (p- C_6F_5), and -166.4 (m- C_6F_5). Data for **5sC**: 1H NMR (CD_2Cl_2): 0.16 (s, 3 H, SiMe), 0.31 (s, 3 H, SiMe), 0.66 (s, 3 H, TiMe), 1.42 (s, 3 H, C_5Me_4), 1.83 (s, 3 H, C_5Me_4), 2.00 (s, 3 H, C_5Me_4), 2.12 (s, 3 H, C_5Me_4), 2.13 (s, 3 H, C_5Me_4), 2.25 (s, 3 H, C_5Me_4), 2.37 (s, 3 H, C_5Me_4), 2.40 (s, 3 H, C_5Me_4), 5.98 (s, 5 H, C_5H_5), 6.15 (s, 5 H, C_5H_5). ^{13}C NMR (CD_2Cl_2): 53.4 (TiMe). ^{19}F NMR (CD_2Cl_2): -133.5 (o- C_6F_5), -162.5 (p- C_6F_5), and -166.4 (m- C_6F_5).

$\{[Ti(\eta^5-C_5H_5)_2(\mu-X)(\mu-\{(\eta^5-C_5Me_4SiMeO)_2(\mu-O)\})][B(C_6F_5)_4]$ ($X = F, 4F-C; Cl, 4Cl-C; Br 4Br-C$). A mixture of **3as** and **3aa** in ca. 1:1 (0.015 g, 0.023 mmol) and 1 equiv of $[Ph_3C][B(C_6F_5)_4]$ (0.021 g, 0.023 mmol) were loaded into a NMR tube, and 0.5 mL of the corresponding solvent CD_2Cl_2 or XC_6D_5 ($X = Br, F$) was added. Each sample was then shaken vigorously, and the reaction was monitored by NMR spectroscopy at $25^\circ C$, showing the

Table 8. Crystallographic Data for $[(TiClCp)_2(\mu-\{(\eta^5-C_5Me_4SiMeO)_2(\mu-O)\})]$ (2aa**)**

formula	$C_{30}H_{40}Cl_2O_3Si_2Ti_2$
fw	671.50
color/habit	orange/prism
cryst dimens (mm ³)	0.26 \times 0.22 \times 0.16
cryst syst	monoclinic
space group	$P2_1/c$
<i>a</i> , Å	12.537(8)
<i>b</i> , Å	15.206(8)
<i>c</i> , Å	16.338(9)
β , deg	101.59(5)
<i>V</i> , Å ³	3051(3)
<i>Z</i>	4
<i>T</i> , K	200
<i>D</i> _{calcd} , g cm ⁻³	1.462
<i>μ</i> , mm ⁻¹	0.808
<i>F</i> (000)	1400
θ range, deg	3.52 to 27.58
index ranges (<i>h</i> , <i>k</i> , <i>l</i>)	$\pm 16, \pm 19, \pm 21$
no. of rflns collected	25 126
no. of indep rflns/ <i>R</i> _{int}	6987/0.1449
no. of obsd rflns (<i>I</i> > 2 σ (<i>I</i>))	4262
no. of data/restraints/params	6987/232/353
<i>R</i> ₁ / <i>wR</i> ₂ (<i>I</i> > 2 σ (<i>I</i>)) ^a	0.0885/0.2215
<i>R</i> ₁ / <i>wR</i> ₂ (all data) ^a	0.1407/0.2561
GOF (on <i>F</i> ²) ^a	1.007
largest diff peak and hole, e Å ⁻³	0.913 and -0.754

$$^a R_1 = \frac{\sum(|F_o| - |F_c|)}{\sum F_o}; wR_2 = \left\{ \frac{\sum [w(F_o^2 - F_c^2)^2]}{\sum [w(F_o^2)^2]} \right\}^{1/2}; GOF = \left\{ \frac{\sum [w(F_o^2 - F_c^2)^2]}{\sum [w(F_o^2)^2]} \right\}^{1/2}$$

formation of **5s-C** and **4X-C** ($X = Cl, Br, F$) in ca. 1:1. Data for **4F-C**: 1H NMR (FC_6D_5): 0.21 (s, 6 H, SiMe), 1.78 (s, 6 H, C_5Me_4), 1.80 (s, 6 H, C_5Me_4), 1.84 (s, 6 H, C_5Me_4), 1.86 (s, 6 H, C_5Me_4), 5.73 (s, 10 H, C_5H_5). ^{13}C NMR (FC_6D_5): -0.1 (SiMe), 11.8, 12.1, 15.1, and 15.6 (C_5Me_4), 119.5–149.4 (C_5Me_4), 119.8 (C_5H_5), 135.4, 138.7, and 149.4 (m, C_6F_5). ^{19}F NMR (FC_6D_5): -53.3 (Ti-F-Ti), -132.7 (o- C_6F_5), -162.8 (p- C_6F_5), and -166.9 (m- C_6F_5). Data for **4Br-C**: 1H NMR (BrC_6D_5): 0.21 (s, 6 H, SiMe), 1.75 (s, 6 H, C_5Me_4), 1.79 (s, 6 H, C_5Me_4), 1.80 (s, 6 H, C_5Me_4), 1.83 (s, 6 H, C_5Me_4), 5.98 (s, 10 H, C_5H_5). ^{13}C NMR (BrC_6D_5): -1.0 (SiMe), 10.8, 11.3, 13.7, and 14.6 (C_5Me_4), 119.5–149.4 (C_5Me_4), 120.2 (C_5H_5), 135.4, 138.7, and 149.4 (m, C_6F_5). ^{19}F NMR (BrC_6D_5): -134.2 (o- C_6F_5), -162.2 (p- C_6F_5), and -166.6 (m- C_6F_5).

Single-Crystal X-ray Structure Determination of Compound 2aa. Suitable single crystals for the X-ray diffraction study were grown from toluene. A crystal was selected, covered with perfluorinated ether, and mounted on a Bruker-Nonius Kappa CCD single-crystal diffractometer. Data collection was performed at 200(2) K. The structure was solved, using the WINGX package,⁶⁸ by direct methods (SHELXS-97) and refined by using full-matrix least-squares against *F*² (SHELXL-97).⁶⁹ All non-hydrogen atoms were anisotropically refined, and hydrogen atoms were geometrically placed and left riding on their parent atoms. SIMU and DELU restraints were applied in this structure. Full-matrix least-squares refinements were carried out by minimizing $\sum w(F_o^2 - F_c^2)^2$ with the SHELXL-97 weighting scheme and stopped at shift/err < 0.001. Crystal data and details of the structure determination are presented in Table 8. Crystallographic data (excluding structure factors) for the structures reported in this paper have been deposited with the Cambridge Crystallographic Data center as supplementary publication no. CCDC-756896 (**2aa**). Copies of the data can be obtained free of charge on application to CCDC, 12 Union Road, Cambridge CB2 1EZ, UK (fax: (+44)1223-336-033; e-mail: deposit@ccdc.cam.ac.uk).

(68) Farrugia, L. J. *J. Appl. Crystallogr.* **1999**, *32*, 837.

(69) Sheldrick, G. M. *SHELXL-97*; University of Göttingen: Göttingen, 1998.

Computational Details. All the theoretical calculations in this article have been performed at the density functional (DFT) level of theory by using the Gaussian 03 program package.⁷⁰ Becke's three-parameter exchange functional (B3)^{71,72} in conjunction with the Lee–Yang–Parr correlation functional (LYP)^{73,74} was employed as implemented in Gaussian 03.

The optimizations were performed with basis set BS1; in this basis set, the lanl2dz effective core potential⁷⁵ has been used to describe the inner electrons of the metal centers (Ti), whereas their associated double- ζ basis set, with an extra series of f functions,⁷⁶ has been employed for the remaining electrons; Si, Cl, O, and C atoms were described with Pople's 6-31G(d) split valence basis set, and H atoms were described with the 6-31G basis set.⁷⁷ In the study of the alkylation reaction with

methyl lithium, the lithium atom and the methyl group were described with a 6-31G(d) basis set, whereas the toluene molecule explicitly introduced was described by the 6-31G basis set.

To approximately account for the effects of the surrounding medium, solvent corrections were calculated in toluene ($\epsilon = 2.379$) as single points at the B3LYP/6-31++G(d,p) level using the conductor-like polarizable continuum (CPCM)⁷⁸ model, in which the cavity is created via a series of overlapping spheres.⁷⁹

Finally, during the studies, it was sometimes necessary to elucidate how the electron density was distributed around the atoms, both the metallic centers, and the substituents. To evaluate this, natural bond orbital analysis (NBO) was performed.^{62,63}

Acknowledgment. We gratefully acknowledge the Spanish MICINN (DGI) (projects MAT2007-60997, CTQ2008-06866-C02-01), Consolider Ingenio 2010 (CSD2007-00006), and DGUI-Comunidad de Madrid (programme S-0505/PPQ-0328, COMAL-CM) (Spain) for financial support. L.P. acknowledges DGUI-CM for a Fellowship. The use of computational facilities of the Centre de Supercomputació de Catalunya (CESCA) is gratefully appreciated.

Supporting Information Available: Crystallographic data for **2aa** and selected NMR spectra. Detailed comparison of the coordination spheres around titanium atoms in compounds of series **2** and **3** and **2** and **B**, discussion on the choice of the model system, highest energy pathways for methylation of **2as**, and Cartesian coordinates and absolute energies of all optimized species. This material is available free of charge via the Internet at <http://pubs.acs.org>.

(70) Frisch, M. J.; Trucks, G. W.; Schlegel, H. B.; Scuseria, G. E.; Robb, M. A.; Cheeseman, J. R.; Montgomery, J., J. A.; Vreven, T.; Kudin, K. N.; Burant, J. C.; Millam, J. M.; Lyengar, S. S.; Tomasi, J.; Barone, V.; Mennucci, B.; Cossi, M.; Scalmani, G.; Rega, N.; Petersson, G. A.; Nakatsuji, H.; Hada, M.; Ehara, M.; Toyota, K.; Fukuda, R.; Hasegawa, J.; Ishida, M.; Nakajima, T.; Honda, Y.; Kitao, O.; Nakai, H.; Klene, M.; Li, X.; Knox, J. E.; Hratchian, H. P.; Cross, J. B.; Adamo, C.; Jaramillo, J.; Gomperts, R.; Stratmann, R. E.; Yazyev, O.; Austin, A. J.; Cammi, R.; Pomelli, C.; Ochterski, J. W.; Ayala, P. Y.; Morokuma, K.; Voth, G. A.; Salvador, P.; Dannenberg, J. J.; Zakrzewski, V. G.; Dapprich, S.; Daniels, A. D.; Strain, M. C.; Farkas, O.; Malick, D. K.; Rabuck, A. D.; Raghavachari, K.; Foresman, J. B.; Ortiz, J. V.; Cui, Q.; Baboul, A. G.; Clifford, S.; Cioslowski, J.; Stefanov, B. B.; Liu, G.; Liashenko, A.; Piskorz, P.; Komaromi, I.; Martin, R. L.; Fox, D. J.; Keith, T.; Al-Laham, M. A.; Peng, C. Y.; Nanayakkara, A.; Challacombe, M.; Gill, P. M. W.; Johnson, B.; Chen, W.; Wong, M. W.; Gonzalez, C.; Pople, J. A. *Gaussian 03, Revision C.02*; Gaussian, Inc.: Pittsburgh, PA, 2004.

(71) Becke, A. D. *J. Chem. Phys.* **1993**, *98*, 5648.

(72) Becke, A. D. *J. Chem. Phys.* **1993**, *98*, 1372.

(73) Stephens, P. J.; Devlin, F. J.; Chabalowski, C. F.; Frisch, M. J. *J. Phys. Chem.* **1994**, *98*, 11623.

(74) Lee, C.; Parr, R. G.; Yang, W. *Phys. Rev. B* **1988**, *37*, 785.

(75) Wadt, W. R.; Hay, P., J. *J. Chem. Phys.* **1985**, *82*, 284.

(76) Ehlers, A. W.; Böhme, M.; Dapprich, S.; Gobbi, A.; Höllwarth, A.; Jonas, V.; Köhler, K. F.; Stegmann, R.; Veldkamp, A.; Frenking, G. *Chem. Phys. Lett.* **1993**, *208*, 111.

(77) Henne, W. J.; Radom, L.; Schleyer, P. v. R.; Pople, J. A., *Ab Initio Molecular Orbital Theory*; Wiley: New York, 1986.

(78) Barone, V.; Cossi, M. *J. Phys. Chem. A* **1998**, *102*, 1995.

(79) Miertus, S.; Scrocco, E.; Tomasi, J. *Chem. Phys. Lett.* **1981**, *55*, 117.